



Available online at www.sciencedirect.com



Precambrian Research 131 (2004) 231–282

**Precambrian
Research**

www.elsevier.com/locate/precamres

Archean crustal evolution in the northern Yilgarn Craton: U–Pb and Hf-isotope evidence from detrital zircons

W.L. Griffin ^{a,b,*}, E.A. Belousova ^a, S.R. Shee ^c, N.J. Pearson ^a, S.Y. O'Reilly ^a

^a Department of Earth and Planetary Sciences, ARC National Key Centre for Geochemical Evolution and Metallogeny of Continents, Macquarie University, Macquarie, NSW 2109, Australia

^b CSIRO Exploration and Mining, North Ryde, NSW 2113, Australia

^c De Beers Australia Exploration Limited, 60 Wilson St., South Yarra, VIC 3141, Australia

Accepted 8 December 2003

Abstract

The integrated application of U–Pb dating, Hf-isotope analysis and trace-element analysis to detrital zircon populations offers a rapid means of assessing the geochronology and crustal evolution history of different terranes within a composite craton. In situ U–Pb and Hf-isotope analyses of 550 zircons from 21 modern drainages across the northern part of the Yilgarn Craton and the adjacent Capricorn Orogen provide a broad view of crustal evolution in Archean and Proterozoic time.

The oldest crustal components (3.7 Ga) are identified in the Yeelirrie geophysical domain [A.J. Whitaker, Proceedings of Fourth International Archean Symposium Ext. Abstracts AGSO-Geoscience Australia Record, vol. 37, 2001, p. 536] that runs N–S down the middle of the craton; these components are represented by ancient zircons and also are reflected in the Hf model ages of younger magmas. Ancient (>3.4 Ga) crust contributed to the generation of younger magmas in the Narryer Province, and the proportion of ancient recycled material increases from east to west across the Murchison Province. In contrast, the Hf-isotope data provide no evidence for crust older than 2.9–3.0 Ga in the Southern Cross or Eastern Goldfields (including the Marymia Inlier) domains. The Yeelirrie domain and the composite Narryer–Murchison block are interpreted as ancient microcontinents, sandwiched with the juvenile terranes of the Southern Cross and Eastern Goldfields domains.

There is little evidence for the existence of a Depleted Mantle reservoir beneath the Yilgarn Craton prior to 3.1–3.2 Ga, but this reservoir is a major contributor to crustal generation from 3.1 to 2.6 Ga; this suggests that much of the continental crust in the craton was generated after ca. 3.2 Ga. 1.8–2.3 Ga magmatism, associated with the Capricorn Orogen, involved the recycling of older crust with little obvious contribution from the Depleted Mantle. A significant (and previously unrecognised) 540 Ma episode in the NE part of the craton involved metamorphism or remelting of the 2.7–3.0 Ga crust of the Eastern Goldfields Province.

© 2004 Elsevier B.V. All rights reserved.

Keywords: Zircons; Hf-isotopes; U–Pb dating; Archean crust; Crustal evolution; Yilgarn Craton

1. Introduction

We can gain insights into the nature of tectonics and crust–mantle interaction in the early Earth by studying the processes of crustal generation in Archean time. This information can help us to evaluate how far the

* Corresponding author. Tel.: +61-2-9850-8954;
fax: +61-2-9850-8943/8428.

E-mail address: wgriffin@laurel.ocs.mq.edu.au (W.L. Griffin).

current plate tectonic paradigm, based on data and observations from Phanerozoic environments, can be projected back in time.

To understand the genesis of a block of crust, we need to know not only the age distribution of the magmatic rocks but also the source (juvenile or recycled) of the magmatic material. The problem commonly has been approached by a combination of U–Pb dating of zircons, and Sm–Nd analysis of their host rocks to define the source materials. This method has several limitations: it is relatively slow and hence expensive, and the Sm–Nd system is prone to metamorphic disturbance with consequent errors in the determination of initial ratios, ε_{Nd} values, and model ages. The problems of Sm–Nd disturbance can be largely circumvented by using the closely related Lu–Hf system, and analysing the Hf-isotope composition of zircon of known U–Pb age. Zircon is very resistant to metamorphic recrystallisation even up to high metamorphic grades, and it essentially preserves the initial $^{176}\text{Hf}/^{177}\text{Hf}$ of its source magma at the time of crystallisation.

This latter approach has been used in several studies of crustal genesis (Patchett et al., 1981; Smith et al., 1987; Vervoort and Patchett, 1996) but until recently has been limited by the need to use zircon composites (which may contain different generations of zircon) in order to obtain enough Hf for analysis. However, the multi-collector ICPMS laser microprobe (LAM-MC-ICPMS) now makes it possible to obtain high-precision Hf-isotope analyses on small portions of single zircon grains (Griffin et al., 2000; Thirlwall and Walder, 1995), while U–Pb ages can be obtained on the same grains by LAM-ICPMS techniques (see below). In addition, trace-element data obtained by electron microprobe analysis and as an adjunct to the U–Pb and Hf-isotope analyses give useful information on the composition of the magma from which each zircon crystallised.

This integration of different analytical datasets makes it possible to survey the magmatic history of a crustal block in terms of age, rock types and sources of material by analysing detrital zircons in sediments derived from that block. In this report, we present the results of a reconnaissance study of zircons taken from modern drainages across the northern part of the Yilgarn Craton and the adjacent Capricorn Orogen. We use these data to evaluate the relative impor-

tance of mantle and crustal sources in the generation of Archean and Proterozoic magmas within major structural provinces of the northern Yilgarn Craton. The magmatic events also mark important tectonic episodes in crustal evolution of the region studied.

2. Regional geological setting

There have been numerous attempts to divide the Yilgarn Craton into provinces, terranes or other major structural units; a review of these is beyond the scope of this paper. In a major synthesis and discussion of previous work, Myers (1993) proposed a series of units with distinct geological histories (Fig. 1). The West Yilgarn Superterrane includes the Narryer terrane in the NW, which contains crust as old as 3.7–3.8 Ga, intruded by 3.0 Ga granitoids, and the Murchison and SW Yilgarn terranes with 3.0 Ga volcanic rocks intruded by 2.9 Ga granitoids. The West Central, East Central and East Yilgarn superterrane are described as containing crust as old as 2.96 Ga. All of the terranes were intruded by large volumes of granitoid rocks between 2.6 and 2.8 Ga.

Whitaker (2001) has proposed a subdivision of the Yilgarn Craton into eight province-sized geophysically distinctive domains (Fig. 2). In the northern part of the craton, these include (from east to west) the Eastern Goldfields, Yeelirrie, Southern Cross, Murchison and Narryer domains. The Yeelirrie domain corresponds roughly to the Barlee terrane of Myers (1993), and the Southern Cross domain takes in the eastern part of Myers' Murchison terrane. We have adopted Whitaker's (2001) domains as a framework for presenting our data, because (as discussed below) they appear to correspond to natural groupings in these data.

The timing of magmatic and metamorphic activity in the Yilgarn Craton has been extensively studied by many groups using SHRIMP ion-probe analysis of zircons (e.g., Nelson, 1997a,b) and many Sm–Nd data are available on the 2.6–2.7 Ga granitoids of the Eastern Goldfields Provinces (Champion and Sheraton, 1997). These data, and inherited cores in zircons, suggest that the dominant high-Cagranitoids of the Eastern Goldfields contain a large juvenile component as well as recycled material 200–300 Ma older ($\varepsilon_{\text{Nd}} = -1.3$ to +2.4). The less abundant low-Cagranitoids show a polarity in ε_{Nd} from –4.5 in the west to +2.0 in the east, sug-

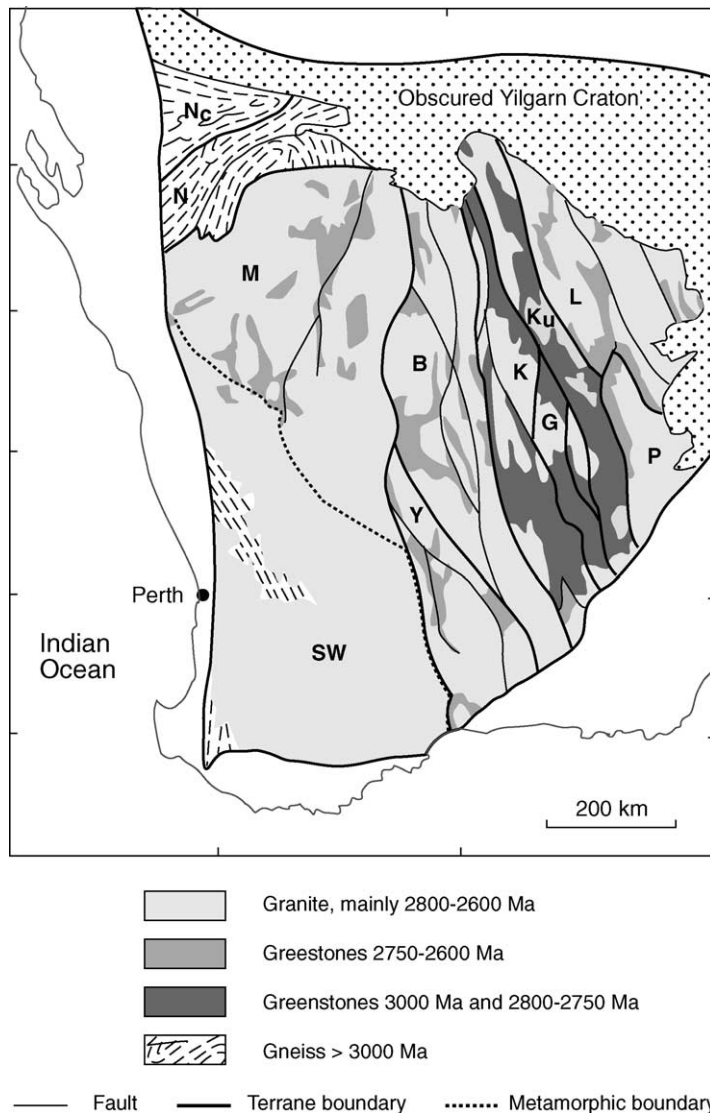


Fig. 1. Terrane structure of the Yilgarn Craton, after Myers (1993). B, Barlee; K, Kalgoorlie; M, Murchison; N, Narryer; Nc, Narryer terrane affected by the Capricorn Orogeny; SW, southwest Yilgarn composite terrane; Y, Yellowdine; Ku, Kurnalpi; G, Gindalbie; L, Laverton; P, Pinjin.

gesting either progressive mixing between older crust and a juvenile source, or a younging of the basement rocks, to the east. However, several ambiguities remain as to the nature and extent of the older crust within the Eastern Goldfields Province (Champion, 1997).

The Proterozoic (1.7–2.2 Ga) Capricorn Orogen lies between the Yilgarn and Pilbara Cratons. Myers (1993) interpreted the orogen as the result of an

oblique collision between these two Archean blocks, accompanied by southward subduction beneath the margin of the Yilgarn. This interpretation contradicts an earlier view (e.g., Gee, 1979) that the Capricorn Orogen represents an intracontinental deformation zone with no evidence for subduction. In Myers' model, the volcanic rocks of the orogen are interpreted as back-arc volcanics, accompanied by the devel-

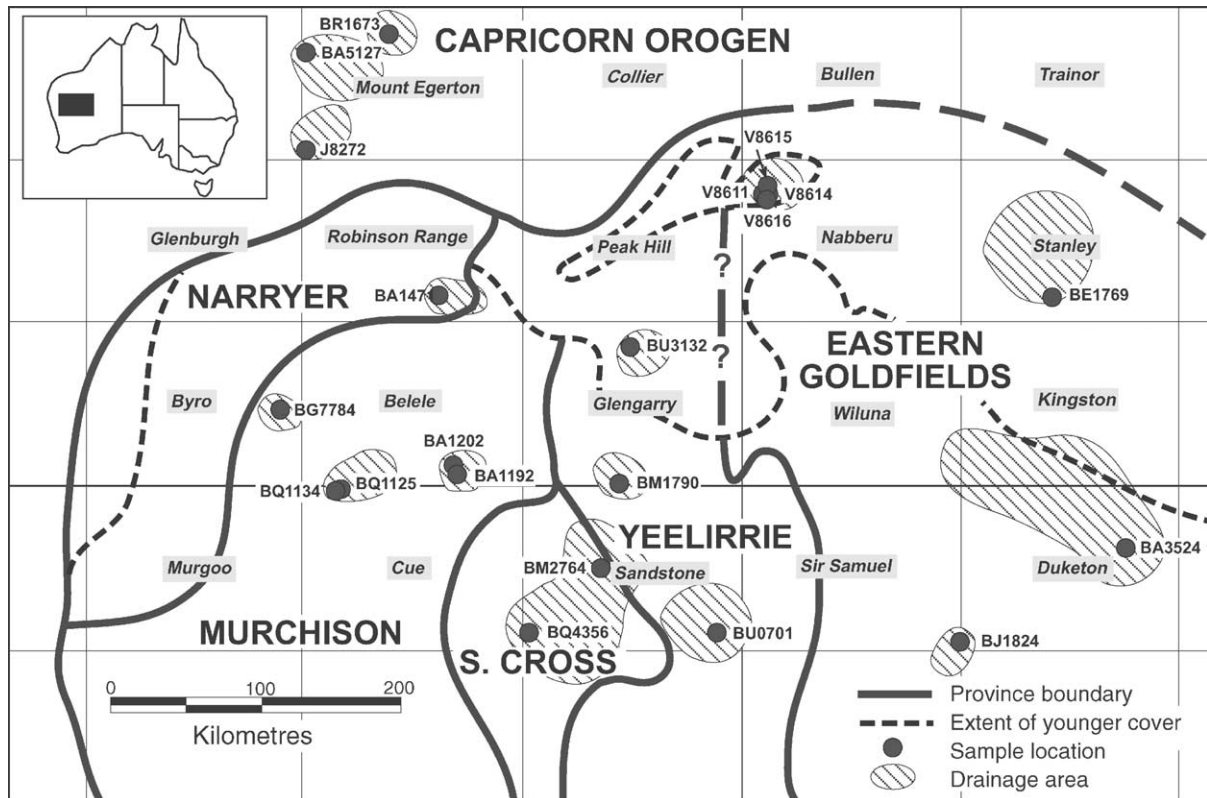


Fig. 2. Sample sites and corresponding drainage areas for this study, with grid lines for 1:250,000 map sheets (names shaded) and the geophysical domains of Whitaker (2001). Map area is shown in black on the index map, upper left.

opment of Cordilleran-type batholiths (2.0–1.8 Ga); these are intruded (1.8–1.7 Ga) by granites formed by crustal melting during the continental collision.

3. Sampling and analytical methods

Trace-element and isotopic (Lu/Hf and U/Pb) in situ analyses were carried out on about 550 zircon grains in this study. The full dataset is available in Appendix A.

Samples are heavy mineral concentrates of sand samples from modern drainages, originally taken by DeBeers Australia Exploration Ltd. for diamond exploration purposes. Sampling covered 21 individual drainages in 15 areas spread across the region of interest; these drainages were selected to give a broad coverage of the different structural domains (Fig. 2), while avoiding overlap between domains as far as possible. The size of the drainages ranges from <500 to

>15,000 km². The relief in the region is generally low, and drainages may have reversed and/or been captured over time. The wide spacing of the samples may offset the confusion that might arise from this problem. The Marymia Inlier (Nabberu area; samples V86–) in the northern part of the craton has been alternatively correlated with the Eastern Goldfields, Murchison and Narryer terranes/provinces (Bagas, 1999).

Zircons were separated from 0.1 to 0.5 mm size fraction of the heavy mineral concentrates; the picking of zircon grains was carried out at the DeBeers laboratories. The separated zircons were sorted under a Leica binocular microscope fitted with UV light, and a representative number of each morphological population recognised was mounted in epoxy blocks and polished for analysis. BSE images, collected in a Camebax SX50 electron microprobe (EMP) at GEMOC, were used to examine internal structures; these observations are summarised in Appendix A. The same EMP

was used to analyse the zircons for Hf and Y contents. This analysis was followed sequentially by analysis of U–Pb ages and Hf-isotope compositions.

3.1. U–Pb dating

U–Pb dating was performed in the GEMOC Key Centre, using a HP 4500 inductively coupled plasma quadrupole mass spectrometer (ICP-MS), attached to a custom-built laser ablation microsampling system (Norman et al., 1996). This incorporates a petrographic microscope that provides a high quality visual image of the sample necessary for U–Pb work.

The analytical procedures for the U–Pb dating are described in detail by Belousova et al. (2001) and Jackson et al. (submitted for publication). A very fast scanning data acquisition protocol was employed to minimise signal noise. Data acquisition for each analysis took 3 min (1 min on background, 2 min on signal). Ablation was carried out in He to improve sample transport efficiency, provide more stable signals and give more reproducible U/Pb fractionation. Provided that constant ablation conditions are maintained, accurate correction for U/Pb fractionation can then be achieved using an isotopically homogeneous zircon standard.

Samples were analysed in “runs” of ca. 20 analyses which included 12 unknown points, bracketed beginning and end, by four analyses of the GEMOC GJ-1 or 02123 zircon standards. The GEMOC GJ-1 zircon standard is slightly discordant with a $^{207}\text{Pb}/^{206}\text{Pb}$ age of 608.5 Ma (F. Corfu, personal communication). The “02123” standard is a gem quality zircon from a Norwegian syenite; it is 295 ± 1 Ma old and

perfectly concordant (Ketchum et al., 2001). Two well-characterised zircons were analysed frequently as an independent control on reproducibility and instrument stability (Table 1; see also Belousova et al., 2001); these analyses demonstrate the accuracy and reproducibility routinely obtained by this method. The effects of minor, short-term variations in elemental fractionation during ablation are incorporated into the errors assigned to the $^{206}\text{Pb}/^{238}\text{U}$, $^{207}\text{Pb}/^{235}\text{U}$ and $^{208}\text{Pb}/^{232}\text{Th}$ ratios (see below).

U–Pb ages were calculated from the raw signal data using the on-line software package GLITTER (www.mq.edu.au/GEMOC). GLITTER calculates the relevant isotopic ratios for each mass sweep and displays them as time-resolved data. This allows isotopically homogeneous segments of the signal to be selected for integration. GLITTER then corrects the integrated ratios for ablation-related fractionation and instrumental mass bias by calibration of each selected time-segment against the identical time-segments of the standard zircon analyses.

Isotope ratios are built from background-subtracted signals for the corresponding isotopes. Uncertainties in these ratios combine the uncertainties of signal and background, arising from counting statistics, added in quadrature. The same propagation is used for unknowns and standards. The standard ratios are interpolated between measurements to estimate the ratios at the time of the measurement of the unknowns. Uncertainties in the standard ratio measurements are propagated through this procedure to estimate the standard ratio uncertainties relevant to each unknown ratio measurement. These relative uncertainties are combined with those for the unknowns in quadrature. A further

Table 1
U–Pb analyses of standard zircons run during this study

Sample	No. of analysis	Ages (Ma)							
		$^{207}\text{Pb}/^{206}\text{Pb}$	2σ	$^{207}\text{Pb}/^{235}\text{U}$	2σ	$^{206}\text{Pb}/^{238}\text{U}$	2σ	$^{208}\text{Pb}/^{232}\text{Th}$	2σ
91500									
LAM-ICPS	71	1064	7	1054	5	1050	6	1064	7
TIMS		1065	1						
Mud Tank									
LAM-ICPMS	35	723	11	728	5	731	5	734	6
TIMS		732	5						

2σ errors on error-weighted means (Ludwig, 2000). References values for standard zircons: 91500: Wiedenbeck et al. (1995), Mud Tank: Black and Gulson (1978).

1% uncertainty (1σ) is assigned to the given values of the isotope ratios for the standard and propagated through the error analysis.

3.2. Common lead corrections

As ^{204}Pb could not be measured due to low signal and interference from ^{204}Hg in the gas supply, the conventional correction for common lead could not be used. Common lead corrections which assume that all discordance is due to common lead (e.g., Ludwig, 2000) will lead to overcorrection when applied to common lead-bearing zircons that have also lost part of their lead in a late event. We therefore have employed the correction procedure of Andersen (2002), which assumes that the observed $^{206}\text{Pb}/^{238}\text{U}$, $^{207}\text{Pb}/^{235}\text{U}$ and $^{208}\text{Pb}/^{232}\text{Th}$ ratios of a discordant zircon reflect a combination of common lead and lead loss at a defined time, and solves the resulting mass-balance equations. The amount of common lead and the common lead-corrected composition of the sample are simultaneously determined. This procedure yields common lead corrections of similar magnitude to those obtained from measurements of ^{204}Pb in ion-probe analysis; the relative error in the amount of common lead is less than 10%. The uncertainty in common lead concentration contributes significantly to the uncertainty in the $^{207}\text{Pb}/^{206}\text{Pb}$ age only above 0.5% common lead. The analyses presented here have been corrected assuming recent lead-loss and a common lead composition corresponding to present-day average orogenic lead as given by the second-stage growth curve of Stacey and Kramers (1975) for $^{238}\text{U}/^{204}\text{Pb} = 9.74$. No correction has been applied to analyses that are concordant within 2σ analytical error in $^{206}\text{Pb}/^{238}\text{U}$ and $^{207}\text{Pb}/^{235}\text{U}$, or which have less than 0.2% common lead. Samples with >2% common Pb have been rejected. Unless otherwise stated, the age data shown in the figures are $^{207}\text{Pb}/^{206}\text{Pb}$ ages for grains older than 1.0 Ga, and $^{206}\text{Pb}/^{238}\text{U}$ ages for younger grains.

3.3. Hf-isotope analyses

Hf-isotope analyses reported here were carried out *in situ* using a New Wave Research LUV213 laser-ablation microprobe, attached to a Nu Plasma multi-collector ICPMS, at GEMOC, Macquarie University. The laser system delivers a beam of 213 nm

UV light from a frequency-quintupled Nd:YAG laser. Most analyses were carried out with a beam diameter of ca. 40 μm , a 10 Hz repetition rate, and energies of 0.6–1.3 mJ per pulse. This resulted in total Hf signals of 1 to 6×10^{-11} A, depending on conditions and the Hf contents. Typical ablation times were 30–120 s, resulting in pits 20–60 μm deep. Ar carrier gas transported the ablated sample from the laser-ablation cell via a mixing chamber to the ICPMS torch. Aside from the use of this laser system, the analytical techniques are those described in detail by Griffin et al. (2000, 2002), these papers also give extensive data on the precision and accuracy of the method.

The Nu Plasma MC-ICPMS has a fixed detector array of 12 Faraday cups; for this work we measured masses 172 and 175–180 simultaneously in static-collection mode. Data were normalised to $^{179}\text{Hf}/^{177}\text{Hf} = 0.7325$, using an exponential correction for mass bias. Initial setup of the instrument was done using a 1 ppm solution of JMC475 Hf, spiked with 80 ppb Yb, which typically yielded a total Hf beam of 10 to 14×10^{-11} A. The laser-ablation analyses were carried out using the Nu Plasma time-resolved analysis software, which allows the more stable portions of the ablation to be selected for analysis, before the data are processed to give the final results. The selected interval is divided into 40 replicates for the calculation of the standard error. Background was collected on peak for 45 s before ablation began.

The measurement of accurate $^{176}\text{Hf}/^{177}\text{Hf}$ ratios in zircon requires correction of the isobaric interferences of ^{176}Lu and ^{176}Yb on ^{176}Hf . This correction is relatively straightforward for the Nu Plasma, because the mass bias of the instrument is independent of mass over the mass range considered here. Interference of ^{176}Lu on ^{176}Hf was corrected by measuring the intensity of the interference-free ^{175}Lu isotope and using $^{176}\text{Lu}/^{175}\text{Lu} = 0.02669$ to calculate the intensity of ^{176}Lu . Similarly, the interference of ^{176}Yb on ^{176}Hf was corrected by measuring the interference-free ^{172}Yb isotope and using $^{176}\text{Yb}/^{172}\text{Yb}$ to calculate the intensity of ^{176}Yb . The appropriate value of $^{176}\text{Yb}/^{172}\text{Yb}$ (0.5865) was determined by successively spiking the JMC475 Hf standard (100 ppb solution) with Yb (10–80 ppb), and determining the value of $^{176}\text{Yb}/^{172}\text{Yb}$ required to yield the value of $^{176}\text{Hf}/^{177}\text{Hf}$ obtained on the pure Hf solution.

Table 2
Analyses of Hf standards

Sample	No. of analyses	Yb (ppm)	Lu (ppm)	Hf (ppm)	$^{176}\text{Lu}/^{177}\text{Hf}$	$^{176}\text{Yb}/^{177}\text{Hf}$	$^{176}\text{Hf}/^{177}\text{Hf}$	$\pm 2\text{S.D.}$	Hf signal (V)
JMC475 Hf	208			0.1–1.0			0.282161	0.000021	5–18 ^a
JMC475 Hf (+Yb)	27	0.04		0.105		0.260	0.282159	0.000060	0.8–4.0
	18	0.01		0.1		0.070	0.282161	0.000040	3.0–4.5
Zircon 91500	60	62.5	13.9		0.00030		0.282297	0.000044	
			12.4 ^b						
TIMS	7		12	5895	0.00029		0.282290	0.000014	
Zircon 61308	45				0.00169	0.04996	0.282999	0.000083	
	12				0.00022	0.00654	0.282966	0.000113	
	22	352	78		0.00138	0.04080	0.282992	0.000093	
TIMS	9		83	5658	0.00247	na	0.282975	0.000050	

Yb and Lu concentrations of zircons by LAM-ICPMS; TIMS data from Wiedenbeck et al. (1995).

^a 5–10v for 0.1 ppm solution using MCN6000; 9–18v for 1 ppm solution using Meinhard nebuliser.

^b Lu calculated from $^{176}\text{Lu}/^{177}\text{Hf}$ and given Hf content.

Repeated analysis of the JMC475 Hf standard solution gives a mean value for $^{176}\text{Hf}/^{177}\text{Hf} = 0.282161 \pm 21$ ($n = 208$). Analysis of this same solution spiked with Yb (Table 2) shows that good precision and accuracy are obtained on the $^{176}\text{Hf}/^{177}\text{Hf}$ ratio, despite the severe corrections on ^{176}Hf ; these analyses include the propagation of error involved in the overlap correction. The JMC475 Hf (100 ppb) + Yb (40 ppb) gave an average $^{176}\text{Hf}/^{177}\text{Hf} = 0.282159 \pm 60$, which demonstrates the robustness of the Yb overlap correction up to $^{176}\text{Yb}/^{177}\text{Hf} = 0.26$. All zircons analysed in this study have much lower $^{176}\text{Yb}/^{177}\text{Hf}$.

The accuracy of the Yb and Lu corrections during LAM-MC-ICPMS analysis of zircon has been demonstrated by repeated analysis of standard zircons with a range in $^{176}\text{Yb}/^{177}\text{Hf}$ and $^{176}\text{Lu}/^{177}\text{Hf}$ (Griffin et al., 2000; Table 2). Analyses of standard zircon 61.308, which has a wide range of $^{176}\text{Yb}/^{177}\text{Hf}$ (0.005–0.065) and $^{176}\text{Lu}/^{177}\text{Hf}$ (0.00016–0.002), show no correlation between these ratios and $^{176}\text{Hf}/^{177}\text{Hf}$ (Table 2). For most zircons >100 μm long, the typical within-run precision (2S.E.) on the analysis of $^{176}\text{Hf}/^{177}\text{Hf}$ is ± 0.00003 , equivalent to an analytical uncertainty of one epsilon unit; on smaller zircons, with shorter run times, larger uncertainties are measured (Appendix A).

The measured $^{176}\text{Lu}/^{177}\text{Hf}$ ratios are used to calculate initial $^{176}\text{Hf}/^{177}\text{Hf}$ ratios. LAM-ICPMS analyses of $^{176}\text{Lu}/^{177}\text{Hf}$ for standard zircon 91500 give $^{176}\text{Lu}/^{177}\text{Hf}$ within error (1σ) of the isotope dilution values (Table 2; Griffin et al., 2000). Standard zircon

61.308 shows a wide range of measured Lu/Hf, and the ID-TIMS value lies within this range (Table 2). These data indicate that Lu and Hf exhibit similar ablation characteristics, and that the $^{176}\text{Lu}/^{177}\text{Hf}$ ratios measured by LAM-MC-ICPMS are not obviously biased. The typical 2S.E. uncertainty on a single analysis of $^{176}\text{Lu}/^{177}\text{Hf}$ is $\pm 1\text{--}2\%$, reflecting both analytical uncertainties and the spatial variation of Lu/Hf across many zircons; at the Lu/Hf ratios considered here (Appendix A), this contributes an uncertainty of $<0.1\epsilon_{\text{Hf}}$ unit.

For the calculation of ϵ_{Hf} values, we have adopted the chondritic values of Blichert-Toft et al. (1997). These values were reported relative to $^{176}\text{Hf}/^{177}\text{Hf} = 0.282163$ for the JMC475 standard, well within error of our reported value (Table 2). To calculate model ages (T_{DM}) based on a depleted-mantle source, we have adopted a model with $(^{176}\text{Hf}/^{177}\text{Hf})_i = 0.279718$ and $^{176}\text{Lu}/^{177}\text{Hf} = 0.0384$; this produces a value of $^{176}\text{Hf}/^{177}\text{Hf} = 0.28325$ similar to that of average MORB over 4.56 Ga. There are currently three proposed values of the decay constant for ^{176}Lu . ϵ_{Hf} values and model ages used in the figures were calculated using the value (1.93×10^{-11} per year); proposed by Blichert-Toft et al. (1997); values for ϵ_{Hf} and model ages calculated using the other two values (1.865×10^{-11} per year, Scherer et al., 2001; 1.983×10^{-11} per year, Bizzarro et al., 2003) are given in Appendix A.

T_{DM} ages, which are calculated using the measured $^{176}\text{Lu}/^{177}\text{Hf}$ of the zircon, can only give a minimum

age for the source material of the magma from which the zircon crystallised. Therefore, we also have calculated, for each zircon, a “crustal” model age (T_{DM}^C) which assumes that its parental magma was produced from an average continental crust ($^{176}\text{Lu}/^{177}\text{Hf} = 0.015$) that originally was derived from the depleted mantle.

3.4. Trace-element discriminants

An extensive study of the trace-element patterns of zircons (Belousova et al., 2002) has shown good correlations between these patterns and the composition of the magmatic host rocks. The zircon database for U, Th, Y, Yb, Lu and Hf, which are acquired during the U–Pb and Hf-isotope analyses, has been evaluated using the CART software (Breiman et al., 1984). This analysis creates a classification tree (Fig. 3a) based on simple binary switches, that allows classification of any individual zircon grain in terms of its rock type. The values of each element at the various switches are well above the detection limits of the different methods used here.

A classification matrix (Fig. 3b) shows that zircons from some rock types can be discriminated with a high degree of probability: zircons from kimberlites, carbonatites, mafic rocks (diabases + basalts), syenitic rocks (syenites, larvikites) and Ne-syenites are recognised with a probability of correct classification >80%. The probability of correct classification for zircons from granitoids (as distinct from other rock types) is >75%, but the division of granitoids by SiO₂ content is more ambiguous. Zircons from granitoids with 65–70% SiO₂ consistently classify as coming from rocks with either higher (40%) or lower (30%) SiO₂ contents. For zircons from the other granitoid classes, the probability of correct classification by SiO₂ group ranges from 49% for those with 70–75% SiO₂, to 63% for those with >75% SiO₂.

In other studies, we have found that zircons from large differentiated mafic sills tend to classify as derived from either mafic rocks or syenites, reflecting their crystallisation from late differentiates. In the present dataset, some samples contain a high proportion of “mafic” zircons, but few “syenitic” ones, and we suspect that many of these “mafic” zircons actually are derived from TTG-suite rocks with low Hf and Y (and HREE) contents (cf. Fig. 3a). Despite

this ambiguity, we find that this tree provides useful information on the broad composition of the source rocks contributing to a detrital zircon sample.

Hoskin and Ireland (2000) suggest that the REE patterns of zircons do not offer a good guide to the composition of their source rocks. However, the data presented here (and in more detail by Belousova et al., 2002) demonstrate that by taking a multivariate approach, and using other elements in addition to the REE, the original host rock type of individual zircon grains can be recognised at a useful degree of confidence. This greatly enhances the use of detrital zircons in provenance studies.

4. Results

The analytical data, and observations on external morphology and internal structure of each grain, are given in Appendix A. Zircons have been distinguished as possibly metamorphic (rather than magmatic) when they display a combination of anhedral or rounded external form, little or no internal structure, low Th and U contents and Th/U < 0.1 (Rubatto et al., 1999; Hoskin and Black, 2000). However, these criteria are not invariably indicative of metamorphic origin, and the identification should be treated with caution.

Because each detrital zircon grain may represent a different source rock, and thus part of the crustal history, grains cannot be selected for perfection, nor arbitrarily rejected for U–Pb discordance. However, the error magnification on the $^{207}\text{Pb}/^{206}\text{Pb}$ age of strongly discordant grains becomes large, and we have rejected a number of such grains. These grains are shown with open symbols in Fig. 4, but are not included in Appendix A. Most of the age populations discussed below are defined by both concordant/near concordant grains, and discordant ones; these are obvious on the inverse-concordia plots in Fig. 4.

4.1. Nabberu area (Marymia Inlier)

The samples (V86–, Fig. 2) come from four small adjacent drainages within the Marymia Inlier, an area of exposed basement surrounded by younger cover rocks. The U–Pb data define a narrow range of $^{207}\text{Pb}/^{206}\text{Pb}$ ages (Figs. 4 and 5) between 2.5 and 2.7 Ga. Thirty-one grains give an error-weighted mean

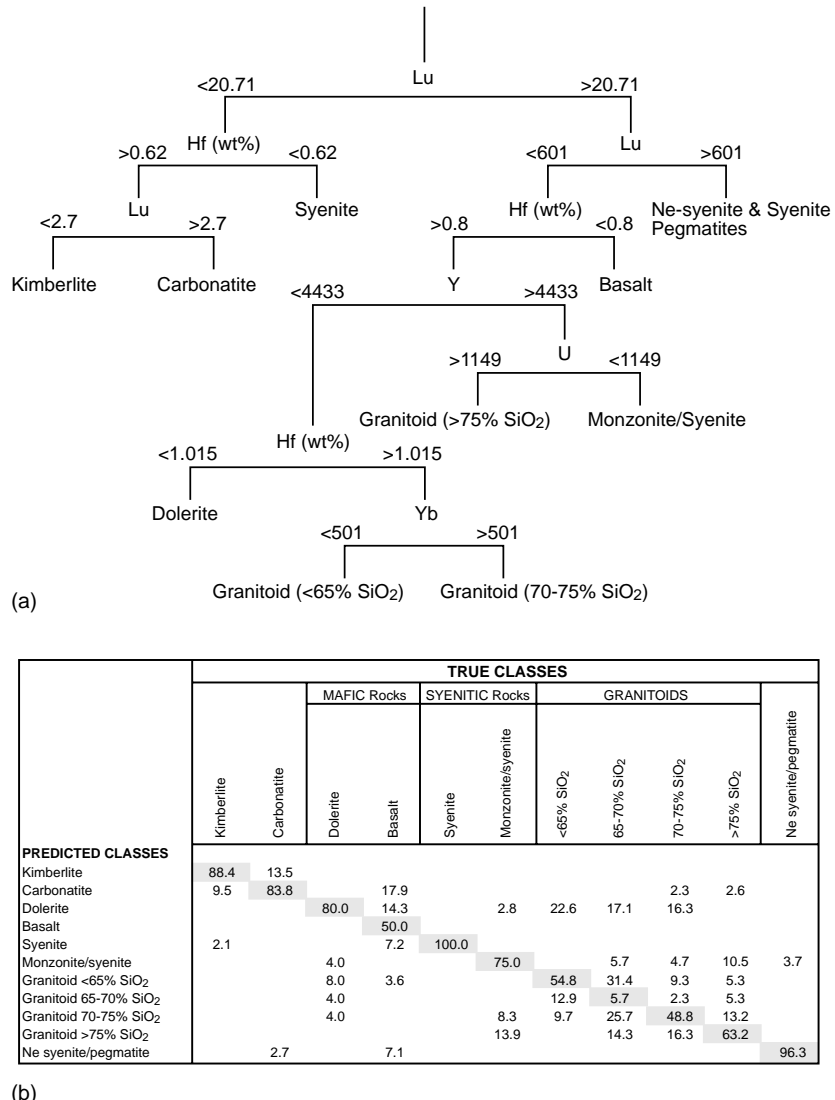


Fig. 3. (a) CART tree for classification of zircons by rock type, using trace and minor elements acquired during EMP, U–Pb and Hf-isotope analysis. (b) CART correlation matrix showing probability of correct classification in a random subset of the zircon database (Belousova et al., 2002).

$^{207}\text{Pb}/^{206}\text{Pb}$ age of 2650 ± 6 Ma, ($\text{MSWD} = 0.76$). The zircons are divided 2:1 between those derived from low-Si granitoids, and those classified as being derived from carbonatites and kimberlites (Fig. 6). Most of the latter are rounded and have little internal structure, as is typical of mantle-derived zircons (Belousova et al., 1999). Most Hf-isotope analyses lie between the CHUR and DM reference lines (Fig. 7),

with ε_{Hf} values from +1 to +8. The mean T_{DM} model age is 2.77 Ga, and the mean T_{DM}^{C} model age is 2.88 Ga. These data provide no evidence for the involvement of crust older than 2.9 Ga in the generation of the zircon-bearing rocks.

The three apparently kimberlitic zircons come from a drainage that heads near the Nabberu-1 kimberlite which has been dated on structural grounds to ≥ 1.9 Ga

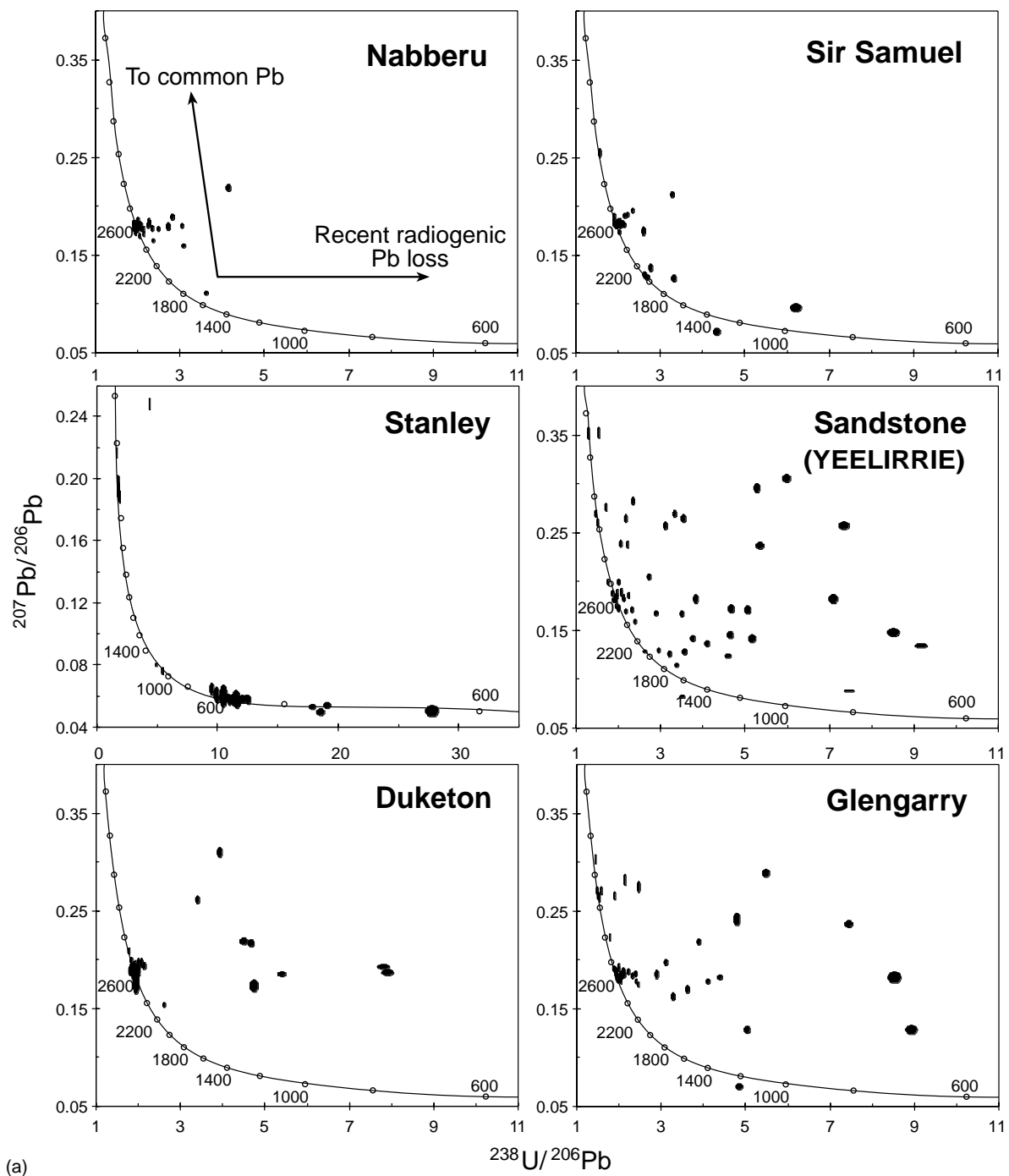


Fig. 4. Inverse concordia plots of U-Pb data for the analysed zircons; data from Appendix A. The effects of common lead contamination and recent lead loss are illustrated by arrows in the Nabberu plot, upper left in (a) and Southern Cross, upper left in (b).

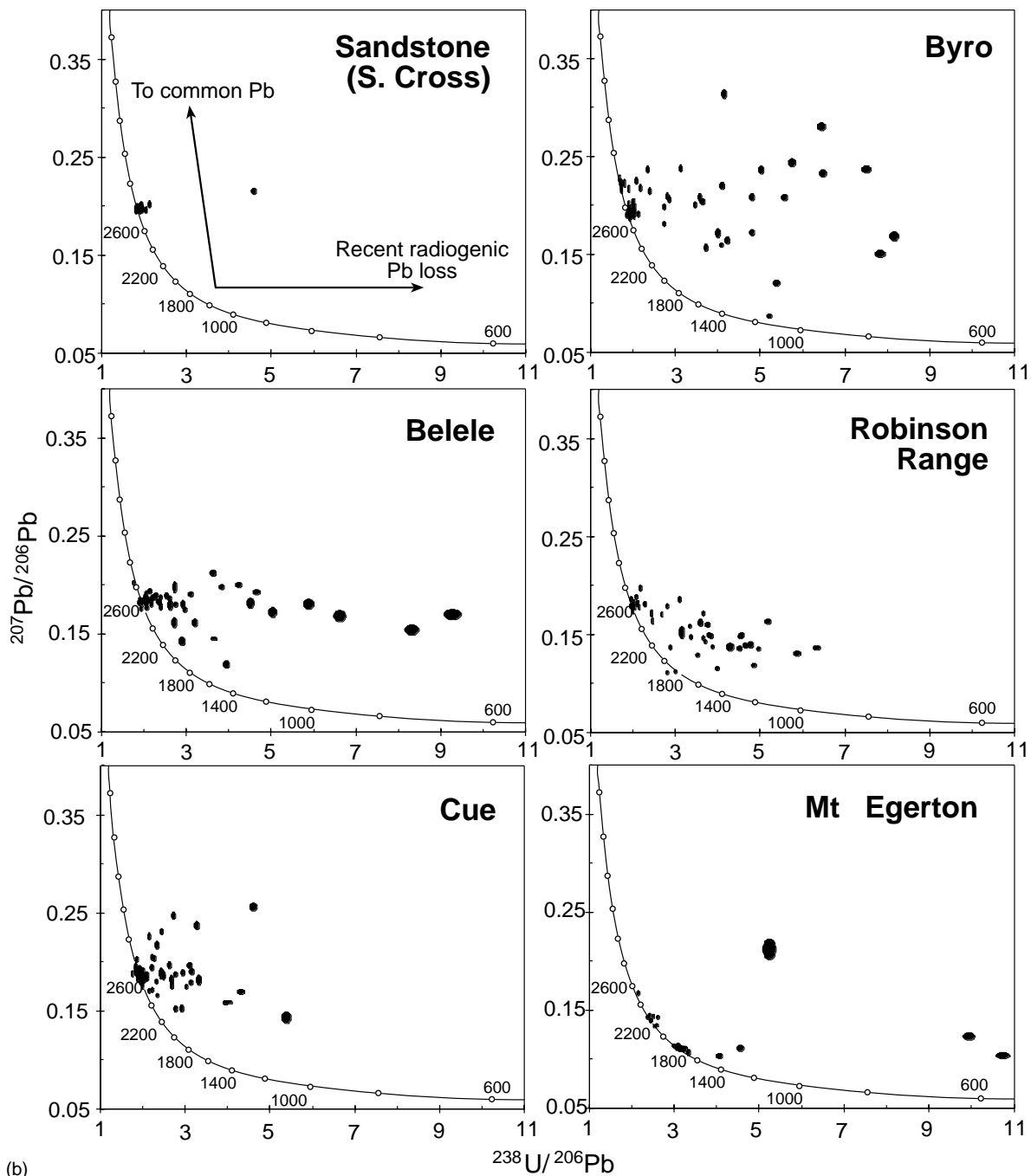


Fig. 4. (Continued).

(b)

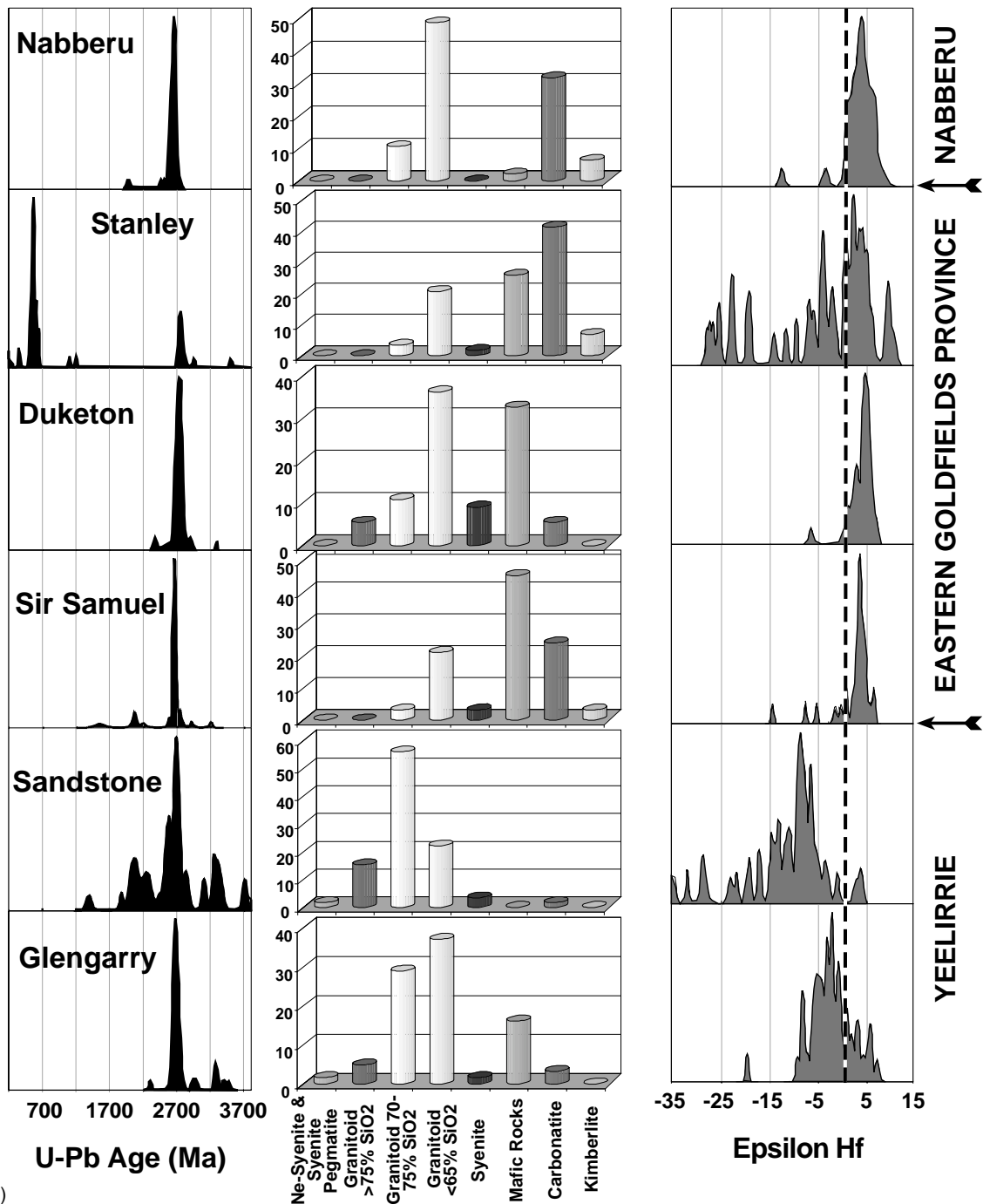


Fig. 5. Left: relative probability plots (Ludwig, 2000) of U-Pb data from each area. Centre: relative abundance of rock types derived from zircon compositions (see Fig. 3). Right: cumulative probability plots of ε_{Hf} data from each area, with vertical bar representing CHUR composition.

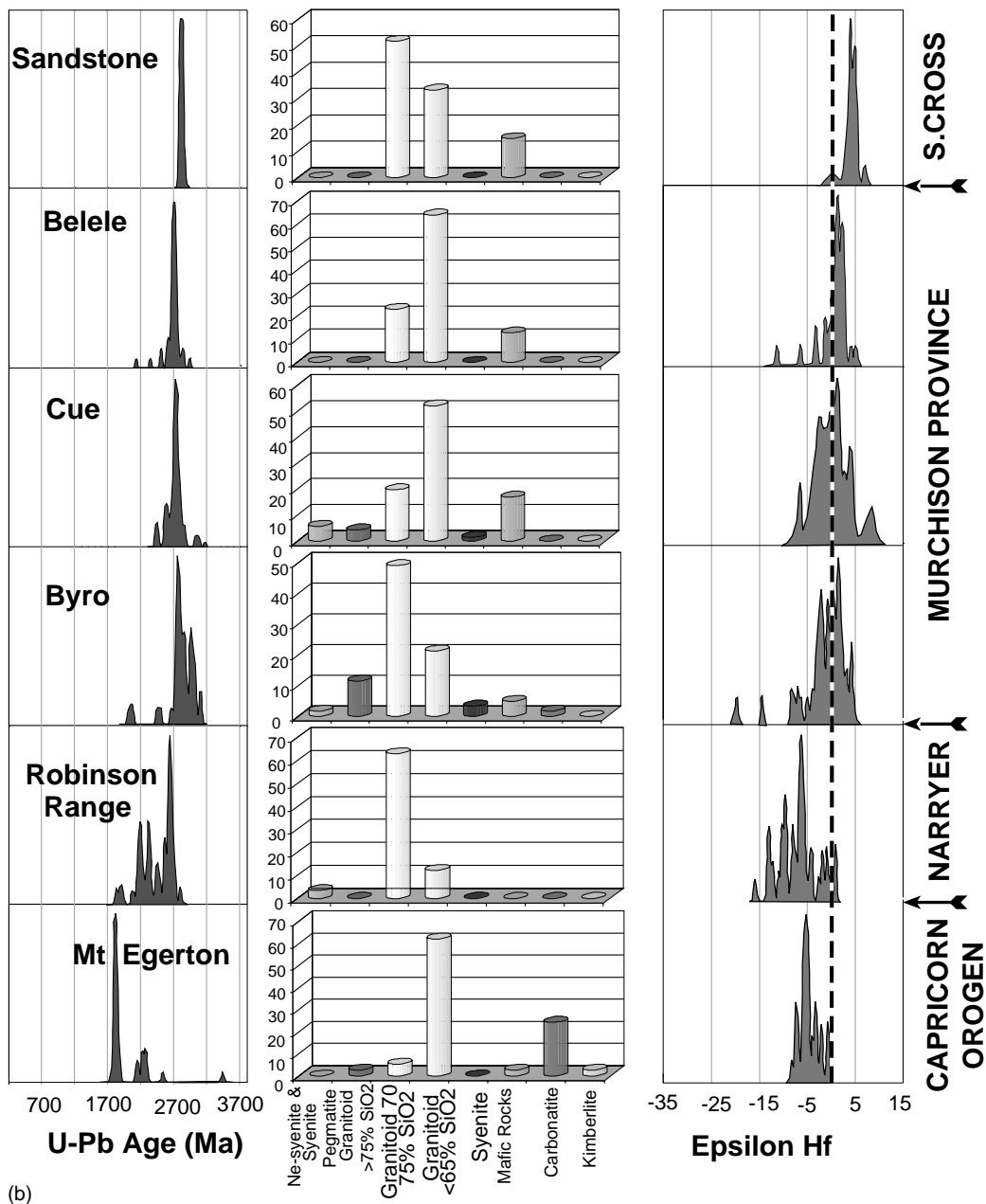


Fig. 5. (Continued).

(Shee et al., 1998). If the Nabberu kimberlites are the source of the zircons, they may be ca. 2.65 Ga old (though kimberlitic zircons may predate the eruption of the kimberlite; Belousova et al., 2001), and related to a group of possibly carbonatitic rocks that have

not been recognised in outcrop and may be deeply weathered. However, no zircons were found during bulk sampling of the Nabberu kimberlites.

Bagas (1999) reported that the Plutonic Well greenstone belt in the Marymia Inlier is intruded by 2.72 Ga

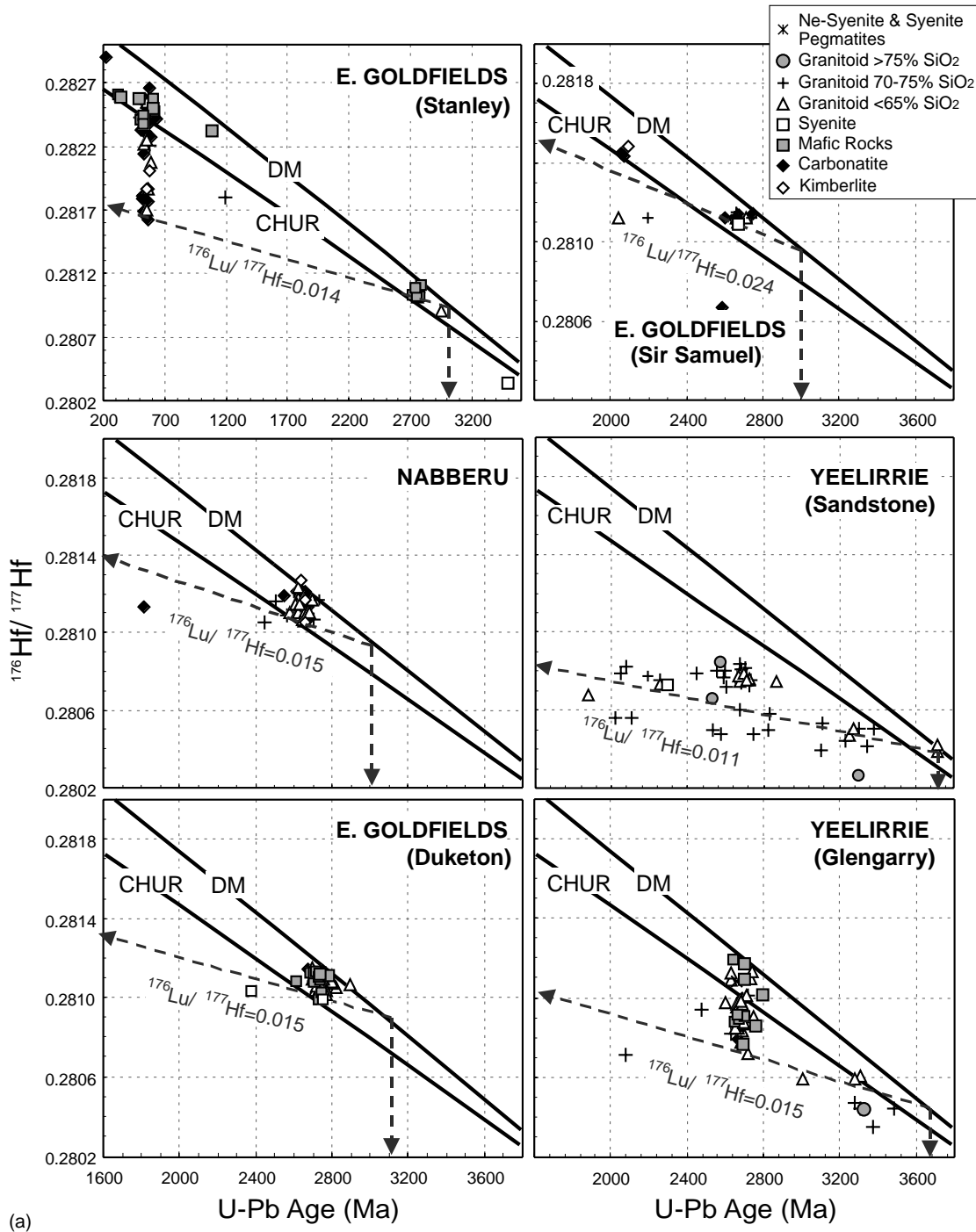


Fig. 6. Plots of $^{176}\text{Hf}/^{177}\text{Hf}$ vs. U-Pb age for the analysed zircons, with each point coded according to rock type. Ages are $^{207}\text{Pb}/^{206}\text{Pb}$ ages for samples with ages >1 Ga, and $^{206}\text{Pb}/^{238}\text{U}$ ages for samples with younger ages.

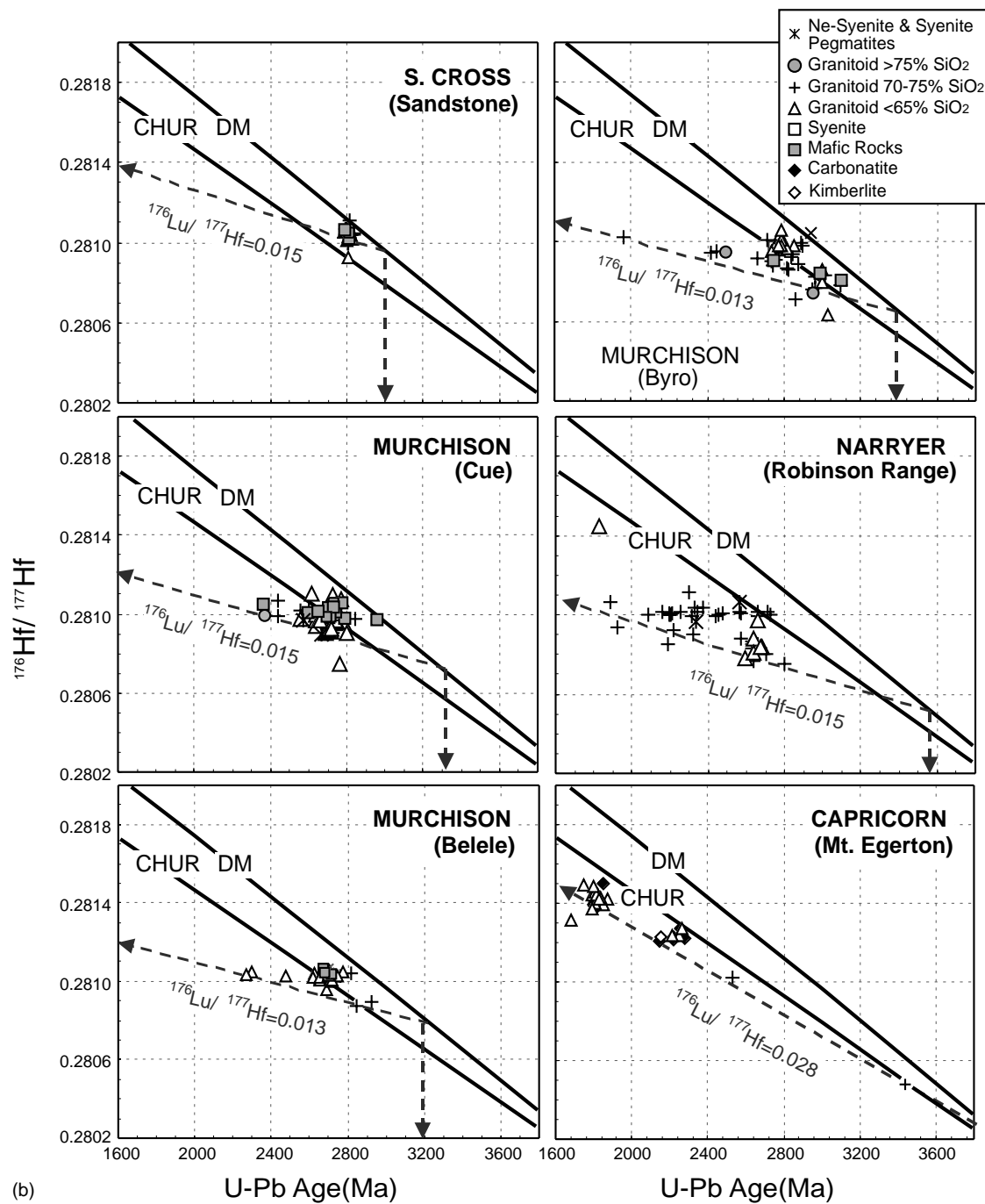


Fig. 6. (Continued).

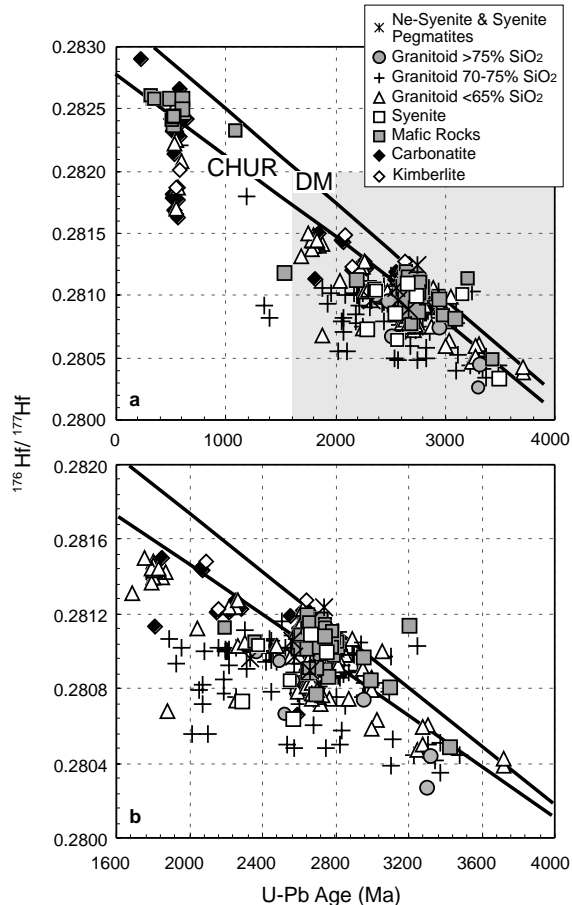


Fig. 7. Composite plot of $^{176}\text{Hf}/^{177}\text{Hf}$ vs. U-Pb age for the analysed zircons, with each point coded according to rock type. (b) An enlargement of the shaded area from (a).

granitoids, 2.69 Ga felsic to intermediate porphyries, and a 2.66 Ga felsic to intermediate porphyry. The majority of the granitoid zircons analysed here may reflect the youngest of these events.

4.2. Eastern Goldfields Province

The sample (BE 1769) from the *Stanley* map sheet in the NE part of the Eastern Goldfields Province contains a large concentration of zircons with $^{206}\text{Pb}/^{238}\text{U}$ ages of 500–600 Ma, with a peak at 542 Ma (Fig. 5). These zircons apparently are derived from a range of rock types, from mafic rocks and carbonatites to granitoids (Fig. 6), and show a large spread in ε_{Hf} , from +9 to −27 (Fig. 7). To our knowledge, the sources of

these zircons have not been recognised in outcrop. A group of ultramafic lamprophyres is known at Buljah Pool in the same general area, but they are reported to be ca. 305 Ma old, based on SHRIMP dating of zircons (Hamilton and Rock, 1990), but Graham et al. (1999) obtained a Re–Os isochron age of 1280 Ma on the rocks, precluding them as a source of the 500–600 Ma zircons. All of these zircons have a rounded morphology and lack internal structure, and many have $\text{Th}/\text{U} < 1$. They may be metamorphic, rather than magmatic, zircons, and may be derived from the younger sediments covering the cratonic basement.

A distinct group of 10 rounded, structureless zircons with very low Th and U contents, but mostly with $\text{Th}/\text{U} > 1$, gives an error-weighted mean $^{207}\text{Pb}/^{206}\text{Pb}$ age of 2747 ± 13 Ma (MSWD = 0.86). Most of these grains classify as derived from mafic rocks, and all have $\varepsilon_{\text{Hf}} = +2$ to +6. Their model ages are only 100–300 Ma older than their crystallisation ages ($T_{\text{DM}}^{\text{C}} = 2.85\text{--}3.0$), which indicates derivation from juvenile sources. Two grains with ages of 3.27 and 3.50 Ga, and $\varepsilon_{\text{Hf}} = -3.3$ and −4.3, respectively, represent the only evidence of older crust in this area. The 540 Ma zircons with the least radiogenic Hf could be derived from 2.75 Ga crust, assuming it has a mean $^{176}\text{Lu}/^{177}\text{Hf} = 0.014$, which is similar to the average continental crust (Fig. 6). The T_{DM}^{C} of these least radiogenic zircons is ≈3.1 Ga. If the zircons are interpreted as magmatic, the large range in ε_{Hf} suggests mixing between this older crust and material derived from the DM source at 540 Ma. However, if these zircons are metamorphic, their spread in ε_{Hf} would simply reflect the evolution of a suite of older rocks with a range in Lu/Hf.

The sample (BA3524) from the *Duketon* map sheet (the drainage extends into the *Kingston* sheet to the north; Fig. 2) defines a tight cluster of ages between 2.7 and 2.75 Ga, with a scatter up to ca. 2.9 Ga; the error-weighted mean $^{207}\text{Pb}/^{206}\text{Pb}$ age of 29 grain = 2745 ± 8 Ma (MSWD = 0.69). Most of the sample is evenly divided between zircons apparently derived from low-Si granitoids and those from mafic rocks. Most zircons can be interpreted as magmatic, but a few are rounded, structureless and have $\text{Th}/\text{U} < 0.5$, and probably are metamorphic. ε_{Hf} lies in narrow range from +1 to +7, and the maximum model ages are only 200 Ma older than the crystallisation ages (mean $T_{\text{DM}} = 2.85$, $T_{\text{DM}}^{\text{C}} = 3.1$). All of the rocks ap-

pear to be derived from juvenile sources, and there is no evidence for the involvement of crust older than 3.1 Ga.

The sample from the *Sir Samuel* map sheet (BJ1824, extending SW into the *Leonora* sheet; Fig. 2) on the western side of the Eastern Goldfields Province shows a major peak in age at 2.6–2.8, dominated by zircons classified as derived from mafic rocks. These are interpreted as igneous; even those with no internal structure have Th/U > 1. Thirty-six grains give an error-weighted mean $^{207}\text{Pb}/^{206}\text{Pb}$ age = 2665 ± 6 (MSWD = 0.43). The mean ϵ_{Hf} of these zircons is +4 (Fig. 7), and their model ages are close to their crystallisation ages (mean $T_{\text{DM}} \approx 2.8$ Ga, mean $T_{\text{DM}}^{\text{C}} \approx 2.9$ Ga), indicating derivation from juvenile sources. One grain with a 2.59 Ga age and very low ϵ_{Hf} has a $T_{\text{DM}} = 3.38$ Ga; this is the only indication of older crust in the area. Five grains give ages of 2.0–2.2 Ga; three classify as kimberlitic or carbonatitic, one as mafic and one as derived from a low-Si granitoid (Fig. 7). They have ϵ_{Hf} from -11.1 to +2.8, and T_{DM}^{C} model ages of 2.5–3.3 Ga.

Myers (1993) listed three periods of granite intrusion (2.68, 2.66, 2.60–2.62 Ga) in the Kalgoorlie terrane, which includes the area sampled by this drainage. More detailed studies (Champion and Sheraton, 1997; Champion, 1997) define a narrower age range, from 2.64 to 2.71 Ga, for all of the Eastern Goldfields Granites. The 2.74 and 2.67 Ga peaks that dominate our samples are consistent with this interpretation, and the mean Hf model ages are similar to those derived from Sm–Nd analysis (2.8–2.9 Ga) of the widespread high-Cagranites (Champion, 1997). The trace-element data suggest that mafic rocks, as well as granitoids, are abundant, but this could represent a misclassification of granitoid-derived zircons with unusually low Hf and Y contents (cf. Fig. 3a); Champion and Sheraton (1997) described a subordinate group of the high-Cagranite suite that is characterised by low Y contents.

4.3. Yeelirrie domain

Three samples were taken within this domain; BU0701 (*Sandstone* sheet) in the southern part, and two drainages in the *Glengarry* sheet to the north. Most of the data in the northern part are from sample BM1790 (Fig. 2).

The sample from the *Sandstone* map sheet is markedly different from the Eastern Goldfields samples. Many zircons give $^{207}\text{Pb}/^{206}\text{Pb}$ ages in the range 3.1–3.7 Ga (Figs. 4 and 5); ϵ_{Hf} ranges from -1 to -12 for those with ages of 3.1–3.4 Ga, and from +2 to +3 for the two 3.7 Ga grains (Fig. 7). The cumulative probability histogram (Fig. 5) shows a large peak around 2.70 Ga, with smaller peaks at 2.59 and 2.95 Ga; all of these zircons are classified as derived from granitoids. Most zircons appear to be magmatic in origin, with the possible exception of the two 3.7 Ga grains. There is a broad scatter of granitoid zircons with ages down to 1.88 Ga, with peaks at 2.1 and 2.28 Ga. All of these have negative ϵ_{Hf} , extending down to -30. The lowest ϵ_{Hf} values at each age can be modelled (Fig. 6) as reflecting remelting of crust 3.7 Ga old, with Lu/Hf = 0.011 (i.e., more felsic than average continental crust). The parental magmas for the main cluster of zircons at 2.7 Ga could be derived from 3.7 Ga crust with $^{176}\text{Lu}/^{177}\text{Hf} = 0.019\text{--}0.025$, or from average crust ($^{176}\text{Lu}/^{177}\text{Hf} = 0.015$) ca. 3.5 Ga old. Both the model ages and the presence of old zircons suggests the reworking of ancient continental crust over a time span of nearly 2 Ga, whereas the low ϵ_{Hf} values give no evidence for the involvement of juvenile mantle sources in the magmatism after ca. 3.3 Ga.

The samples from the northern part of the domain (*Glengarry* sheet) also contain a population of zircons ranging back to 3.4 Ga, with $\epsilon_{\text{Hf}} \approx +1$ to -7. Many of these are rounded, but their internal structures, wide range in Th and U, and Th/U > 1 indicate a magmatic origin. The dominant age peak is at 2.65–2.7 Ga, and one group ($n = 25$) gives an error-weighted mean $^{207}\text{Pb}/^{206}\text{Pb}$ age = 2680 ± 7 Ma (MSWD = 0.75). The inferred rock types of this group range from mafic to granitic, but are mainly low-Si granitoids. ϵ_{Hf} is bimodally distributed, with one group from +1 to +6, and the others from -0.5 to -9. Although this peak age is similar to those from the Eastern Goldfields Province, the distribution of ϵ_{Hf} is significantly different (Fig. 6). The least radiogenic Hf-isotope compositions in the 2.68 Ga group could be generated from average continental crust 3.6–3.7 Ga old (Fig. 7). The spread in ϵ_{Hf} implies the participation of a Depleted Mantle source as well, and mixing between these sources at 2.68 Ga. One zircon from a high-Si granitoid gives an age of 2.1 Ga, and a low ϵ_{Hf} (-25).

The samples from the northern and southern parts of the domain record a similar series of events, but with different relative abundances of zircon. The main differences are the higher proportion of zircons apparently derived from mafic rocks, and the contribution of a Depleted Mantle component to the ≈ 2.7 Ga magmatic event, in the northern part of the domain; the two effects are likely to be related. The zircons from the southern part of the domain appear to be derived mainly from high-Si granitoids, whereas these are less abundant in the northern part.

4.4. Southern Cross domain

The zircons analysed from this province come from two large adjacent drainages (samples BM2764, BQ4356). Both are dominated by zircons apparently derived from granitoids, equally divided between low- and high-Si types, and nearly all of these are interpreted as magmatic zircons on the basis of their internal structures and Th/U. The data define a single age peak with an error-weighted mean $^{207}\text{Pb}/^{206}\text{Pb}$ age = 2807 ± 6 Ma ($n = 29$; MSWD = 0.79). They show a narrow range in ε_{Hf} at $+4.1 \pm 2.2$ (2σ ; Fig. 7); this approaches the isotopic composition of the model Depleted Mantle at this time (+6.7). The mean T_{DM}^{C} = 2.97 Ga; there thus is no evidence in these data for the existence of continental crust older than 3.0 Ga in the domain.

4.5. Murchison Province

The samples (BA1202, BA1192) from the *Belele* map sheet on the eastern side of the Province show a major peak at ca. 2.7 Ga, with a shoulder at 2.62 Ga. The oldest analysed zircon gives an age of 2.93 Ga. The samples are dominated by magmatic zircons from “low-Si granitoids”, most with $\varepsilon_{\text{Hf}} > 0$ but below the Depleted Mantle curve (main cluster 0 to +4). There is a scatter of zircons with ages down to 1.95 Ga, but showing the same range of Hf-isotope composition as the older grains. These grains have diffuse internal structures or show no zoning on the BSE images, and most have Th/U < 1; they are interpreted as metamorphically recrystallised zircons. Most T_{DM}^{C} model ages are equal to 3.1 Ga, and only one is as high as 3.2 Ga. There is thus no evidence for crust older than ca. 3.2 Ga in this area.

In the middle of the Province, zircons from the northern edge of the *Cue* map sheet and the southern edge of the *Belele* sheet (samples BQ1125, BQ1134) define a broad peak in ages from 2.5 to 2.8 Ga; these zircons appear to be magmatic, and derived mainly from low-Si granitoids, and some mafic rocks. One group ($n = 27$) gives an error-weighted mean $^{207}\text{Pb}/^{206}\text{Pb}$ age = 2724 ± 7 Ma, (MSWD = 0.66); ε_{Hf} ranges from -3 to +5 for most of these (Fig. 6). There is a scatter of younger grains between 2.35 and 2.45 Ga, with a wide range in ε_{Hf} . The least radiogenic Hf in zircons with ages of 2.3–2.7 Ga can be produced from an average continental crust extracted from the Depleted Mantle at 3.3–3.4 Ga (Fig. 6); one grain with lower ε_{Hf} gives $T_{\text{DM}}^{\text{C}} = 3.65$ Ga. There is an obvious Depleted Mantle component to the 2.7–2.9 magmatism, but this is not apparent in zircons with ages <2.65 Ga.

The sample from the *Byro* map sheet on the western edge of the Province (BG7784) shows a broader age range, more weighted toward older ages. The zircons show generally high Th and U contents and most have Th/U > 1, suggesting a magmatic origin. The cumulative probability histogram (Fig. 5) shows major peaks at 2.76, 2.85, 2.94 and 3.01 Ga. The oldest zircons are two grains with ages of 3.1 Ga. In contrast to the samples from the eastern part of the Province, this one is dominated by zircons from silicic granitoids, and there are few that classify as derived from mafic rocks. The distribution of inferred rock types is similar to that of the southern Yeelirrie domain (Fig. 6). Most of the main group of zircons have ε_{Hf} from -5 to +5. One Capricorn-age zircon (1.97 Ga) has $\varepsilon_{\text{Hf}} = -16.8$; one 1.35 Ga grain has $\varepsilon_{\text{Hf}} = -34$. The oldest T_{DM}^{C} model ages are 3.5–3.7 Ga; the range of ε_{Hf} displayed by the 2.7–2.9 Ga magmatism suggests interaction between this older crust and the Depleted Mantle source.

Myers (1993) described the crust of the Murchison Province in terms of an older granite-greenstone complex with 3.0 Ga ages, intruded by 2.90 Ga granites. Nutman et al. (1993) gave ages of 2.9–3.0 Ga for gneisses along the eastern side of the Province. A younger granite-greenstone complex is dated at ca. 2.80 Ga, with monzogranite intrusion at 2.69–2.68 Ga, and intrusion of granites, granodiorites and tonalites around 2.63 Ga. Wang et al. (1998) reported SHRIMP ages of 2.94–2.96 Ga for felsic volcanics at Golden

Grove, and 2.81 Ga in an overlying sequence. Similar ages for these units have been reported in the Mt. Magnet and Meekatharra areas (Wang et al., 1996). Wiedenbeck and Watkins (1993) also recognised two greenstone sequences, one at 2.9–3.0 Ga and another at ca. 2.76 Ga; Schiøtte and Campbell (1996) found ages of 2.7–2.75 Ga for the younger sequence. Younger granites in the western part of the province have been dated at 2.62–2.72 Ga, and these granites have Nd model ages of 3.0–3.3 Ga (Nutman et al., 1993).

The older age groups are best represented in the sample from the *Byro* sheet. The 2.70–2.76 Ga zircons with high ε_{Hf} , which are important in all three sample areas within the Province, appear to correspond to the younger greenstone sequence. The Hf data suggest that older crust has contributed to the major magmatism at 3.0–2.6 Ga, and that this contribution increases westward toward the Narryer Province. This is consistent with the Nd isotope evidence for the involvement of 3.0–3.3 Ga crust in the late Archean granitoids on the western edge of the Province (Nutman et al., 1993).

4.6. Narryer Province

The zircons from one sample (BA1174) in the *Robinson Range* map sheet are derived mainly from “silicic granitoids”. They show a wide range in ages from 1.84 to 2.8 Ga; the major age peaks are at 2.20, 2.33, and 2.65 Ga. The latter peak gives an error-weighted mean $^{207}\text{Pb}/^{206}\text{Pb}$ age = 2647 ± 9 Ma (MSWD = 0.67, n = 13), suggesting derivation from a single source. The ε_{Hf} values of zircons with ages of 2.6–2.7 Ga range from +1 to −10. A cluster of grains with ages of 1.9–2.35 Ga probably reflects the magmatism of the Capricorn Orogeny. However, some of these are rounded and have Th/U < 0.5, and may be metamorphic. The 1.9–2.35 zircons have low ε_{Hf} (−5 to −18), and T_{DM}^{C} model ages of 3.3–3.8 Ga indicating a crustal derivation. Most of the Hf-isotope data can be modelled as the product of remelting (or metamorphism) of average crust with ages from 3.0 to 3.6 Ga (Fig. 6; see T_{DM}^{C} ages), or 3.5 Ga crust with a range in $^{176}\text{Lu}/^{177}\text{Hf}$ from 0.015 (average crust) to 0.027 (mafic crust). There is no requirement for input from a Depleted Mantle source after 2.7 Ga.

Myers (1993) regarded the Narryer Province crust as the oldest part of the Yilgarn block, citing evidence from SHRIMP studies for 3.73 Ga tonalites, 3.60–3.68 granites and 3.73 layered mafic-ultramafic complexes, as well as 3.40 Ga granites and 3.30 Ga metamorphism. Nutman et al. (1993) dated a number of gneiss units in the eastern part of the Province at 3.3–3.73 Ga. None of these old ages are found in zircons from our sample, although the young granitic zircons in the sample contain isotopic evidence for such old crust. The Hf model ages of 3.0–3.6 Ga for these rocks are consistent with the Nd model ages of 3.2–3.7 Ga on basement gneisses, reported by Nutman et al. (1993). The lack of older zircons in our sample may be related to its position on the southern margin of the Province.

4.7. Capricorn Orogen

Three samples from the *Mt. Egerton* map sheet (J8272, BA4127, BR1673) lie within the Capricorn Orogen along the northern edge of the Yilgarn Craton. Most of the zircons are highly rounded, but oscillatory zoning and high Th/U suggest that most of them are magmatic in origin. Old crust is represented by one age at 2.5 Ga, and one at 3.4 Ga. Nearly half the grains analysed (n = 19) define a peak with an error-weighted mean $^{207}\text{Pb}/^{206}\text{Pb}$ age = 1813 ± 8 Ma (MSWD = 0.42). This is similar to the ages reported for felsic volcanics and syntectonic granites (1.80–1.82 Ga) in this region (Occhipinti et al., 1998; Hall et al., 2001; references therein).

Most of the remaining zircons fall into two peaks at ca. 2.16 and 2.25 Ga. The samples are dominated by zircons apparently derived from low-Si granitoids, but a few are classified as being derived from carbonatites. All fall into a narrow range of $\varepsilon_{\text{Hf}} < 0$, which implies derivation from older crust. T_{DM}^{C} ages are ca. 2.7 Ga for the younger group, and 2.9 Ga for 2.1–2.3 Ga group. A mafic (mean $^{176}\text{Lu}/^{177}\text{Hf} = 0.025$) juvenile crust equivalent in age to the oldest analysed zircon (3.44 Ga), or a 3.6–3.8 Ga mafic crust with a mean $^{176}\text{Lu}/^{177}\text{Hf} = 0.028$, could produce the mean ε_{Hf} observed at each younger age. If the crust is assumed to be more felsic, an input from the Depleted Mantle would be required in each time slice; however, the narrow spread in ε_{Hf} within each group argues against this model.

5. Discussion

5.1. Appearance of the Depleted Mantle reservoir

The Depleted Mantle reservoir is broadly complementary to the continental crust, and the earliest appearance of this reservoir is an important parameter in understanding the evolution of the early Earth. Most zircons older than 3.2 Ga analysed in this study have $\varepsilon_{\text{Hf}} = 0$ (Fig. 7); they crystallised from magmas with Hf-isotope compositions similar to the chondritic unfractionated reservoir (CHUR), or from magmas derived from older crust. The two oldest grains are from the Yeelirrie Province. They have $^{207}\text{Pb}/^{206}\text{Pb}$ ages of 3716 ± 32 and 3717 ± 34 (2σ), classify as being derived from low-Si granitoids, and have $\varepsilon_{\text{Hf}} = 2.9 \pm 1$ and 4.2 ± 0.7 (2σ) corresponding to the model Depleted Mantle at that time. They are above the CHUR value at the 4σ level, and may represent the earliest appearance of the DM reservoir in this area. However, if the recently proposed value for the decay constant of ^{176}Lu (Scherer et al., 2001) is used, their ε_{Hf} values become +1 and +2, respectively, and this makes their status as representatives of the Depleted Mantle more ambiguous. The internal structures of these two grains, and their low Th/U, suggest that they are metamorphic rather than magmatic, and they therefore should not be used to assess the isotopic composition of 3.7 Ga magmas.

Excluding these two grains, there is no evidence for the presence of the Depleted Mantle reservoir before 3.2 Ga. This is consistent with the data of Amelin et al. (1999), who found no $\varepsilon_{\text{Hf}} > 0$ in zircons as young as 3.4 Ga from the Jack Hills quartzite (Narryer Province). These observations suggest that large volumes of continental crust had not been isolated from the convecting upper mantle prior to ca. 3.2 Ga, at least beneath what is now the Yilgarn Craton. This is similar to the age derived by Smith et al. (1987) for the appearance of the Depleted Mantle reservoir in the southern Superior Province, Canada.

May grains younger than 3.2 Ga fall on or above the DM curve (Figs. 6 and 7). The best evidence for 3.0–3.2 Ga Depleted Mantle is from the Murchison Province; $\varepsilon_{\text{Hf}} > 0$ is found mainly in zircons from mafic rocks and low-Si granitoids. The DM source contributed significantly to magmatism in the Murchison, Southern Cross and Eastern Goldfields domains

from 2.9 to 2.6 Ga. After that, it was not an important factor in crustal magmatism in the Yilgarn Craton for at least 1 Ga, despite evidence of magmatism at 1.8 and 2.3–2.0 Ga.

5.2. Early crustal generation in the Yilgarn Craton

The zircon ages and the Hf-isotope data can be used to evaluate the age of the earliest crustal rocks in each domain. There is only a low probability of finding a small inherited or recycled zircon population, such as the ancient zircons from the Jack Hills Quartzite (Amelin et al., 1999; Wilde et al., 2001; references therein) with the type of sampling used in this study (Nutman, 2001). However, the initial Hf-isotope compositions of the zircons can provide strong constraints on the presence of ancient continental crust at depth.

The oldest crust identified in this study is found in the Yeelirrie domain. Individual zircons give $^{207}\text{Pb}/^{206}\text{Pb}$ ages back to 3.7 Ga in the southern part of the domain, and material of this age appears to have made a major contribution to later magmatic rocks. The oldest zircons identified from the northern part are 3.4 Ga old, but modelling of the Hf-isotope compositions of the 2.6–2.8 Ga magmatic zircons suggests their parental magmas were derived from 3.6 to 3.7 Ga continental crust.

While the old zircons could be derived from old sandstones (D. Nelson, personal communication), and ultimately from another terrane such as the Narryer block to the NW, the low ε_{Hf} values of many zircons from 2.6 to 2.8 Ga magmatism require the presence of similarly ancient crust at depth. We also regard it as significant that the distribution of these signatures of ancient crust corresponds to the Yeelirrie domain defined on geophysical criteria (Whitaker, 2001). We therefore suggest that this domain represents a micro-continent with crust = 3.5 Ga old. The existence of this ancient block between the Murchison and Eastern Goldfields Provinces has not been recognised previously (Myers, 1993). It may be the “distant cratonic source” of 2.9–3.57 Ga zircons found in metasedimentary sequences within the Eastern Goldfields Province (Krapez et al., 2000).

The oldest zircons from the Narryer Province analysed in this study are only ca. 2.8 Ga, and our sampling clearly is not representative of the province as a whole. As noted above, this may reflect the position

of our sample on the southern margin of the Province; in addition, some older zircons may have been destroyed during transport. Nevertheless, modelling of the Hf-isotope data suggests that the host magmas of the analysed zircons were derived by remelting of continental crust at least 3.4 Ga old. This is consistent with SHRIMP zircon ages of 3.6–3.7 Ga from basement rocks in the province (Myers, 1993).

In the Murchison Province, the oldest zircon age in our samples is 3.17 Ga. However, there appears to be a gradation in mean crustal age across the province; the oldest crustal model ages vary from 3.1 to 3.2 Ga in the east, to ca. 3.3–3.4 Ga in the centre of the province, to 3.5–3.7 Ga in the western part. This pattern suggests either an overall younging of the crust, or an increasing degree of interaction between the older crust and the Depleted Mantle, eastward across the Province. However, even the eastern edge of the province has model ages significantly older than those found in the adjacent Southern Cross domain; this is consistent with the Nd model ages reported in the eastern part of the Province by Nutman et al. (1993).

The samples from the Southern Cross domain, the Eastern Goldfields Province and the Marymia Inlier are dominated by zircons from 2.6 to 2.8 Ga mafic to granitic rocks. The Hf-isotope compositions of most are consistent with derivation from the Depleted Mantle reservoir; the oldest model ages (T_{DM}^C) are ≈ 3.1 Ga. Three zircons with ages of 2.9–2.95 Ga may be derived from this crust. There is no isotopic evidence in our data for older crust beneath the Eastern Goldfields Province, except for two 3.3–3.5 Ga zircons from the Stanley sheet. The data from the Marymia Inlier are similar in age and Hf-isotope signature to those from the Eastern Goldfields, and distinct from the signatures of the 2.6–2.8 Ga magmatism in the Narryer and Murchison Provinces. This similarity suggests that at least the eastern part of the inlier is correlative with the Eastern Goldfields Province.

The zircon data from this study indicate that the Yeelirrie domain and the Narryer Province are the oldest parts of the Yilgarn Craton. The apparent gradation in crustal model ages across the Murchison Province may be evidence that it was progressively accreted to the Narryer terrane, so that the ancient Narryer core grew to the S.E. Nutman et al. (1993) concluded that the Narryer Province was thrust over the Murchison

block at 2.7–2.8 Ga; we suggest that this may have been the final stage in the tectonic development of the two provinces. The Yeelirrie domain and the composite Murchison–Narryer domain would then represent older crustal fragments, sandwiched between the juvenile terranes of the Southern Cross domain and the Eastern Goldfields Province during the amalgamation of the Yilgarn Craton.

5.3. Late Archean magmatism (2.6–2.8 Ga)

The widespread and voluminous 2.6–2.8 Ga magmatism in the Yilgarn Craton commonly is considered to be related to the assembly of the craton, part of a “major episode of plate tectonic activity which swept together and amalgamated a number of diverse crustal fragments—including volcanic arcs, back arc basins, and microcontinents—to form the Yilgarn Craton” (Myers, 1993).

The age of this major episode shows a lateral variation within and between provinces that may be significant, though a better evaluation will require more closely spaced data. The major peak of felsic magmatism recorded in our samples is 2.74–2.76 Ga in the eastern part of the Eastern Goldfields Province, and 2.66 Ga in the western part. Nelson (1997a,b) noted that the 2.66 Ga age corresponds to the major peak of SHRIMP data on granitic rocks from the eastern part of the craton, and commented that “relatively few granitoid bodies older than 2675 Ma have been identified”. However, he mentions a 2738 Ma deformed granitic gneiss in the northern part of the province, and older rocks are known. These may be more widely distributed in the eastern part of the craton than was previously recognised; the Stanley and Duketon samples each represent very large drainage areas (Fig. 2).

2.65 Ga also is the dominant age in the samples from the Nabberu area; this age and the Hf-isotope data are consistent with a correlation between the Marymia Inlier and the western part of the Eastern Goldfields Province. In the Yeelirrie domain the late magmatism peaks at 2.68–2.70 Ga, whereas it peaks at 2.8 Ga in the Southern Cross domain. In the Murchison Province there is a gradient from 2.70 Ga in the eastern part, to 2.73 Ga in the centre, to 2.76 Ga in the west, which may be significant. The late magmatism in the Narryer Province peaks at 2.65 Ga; this is identical to the age

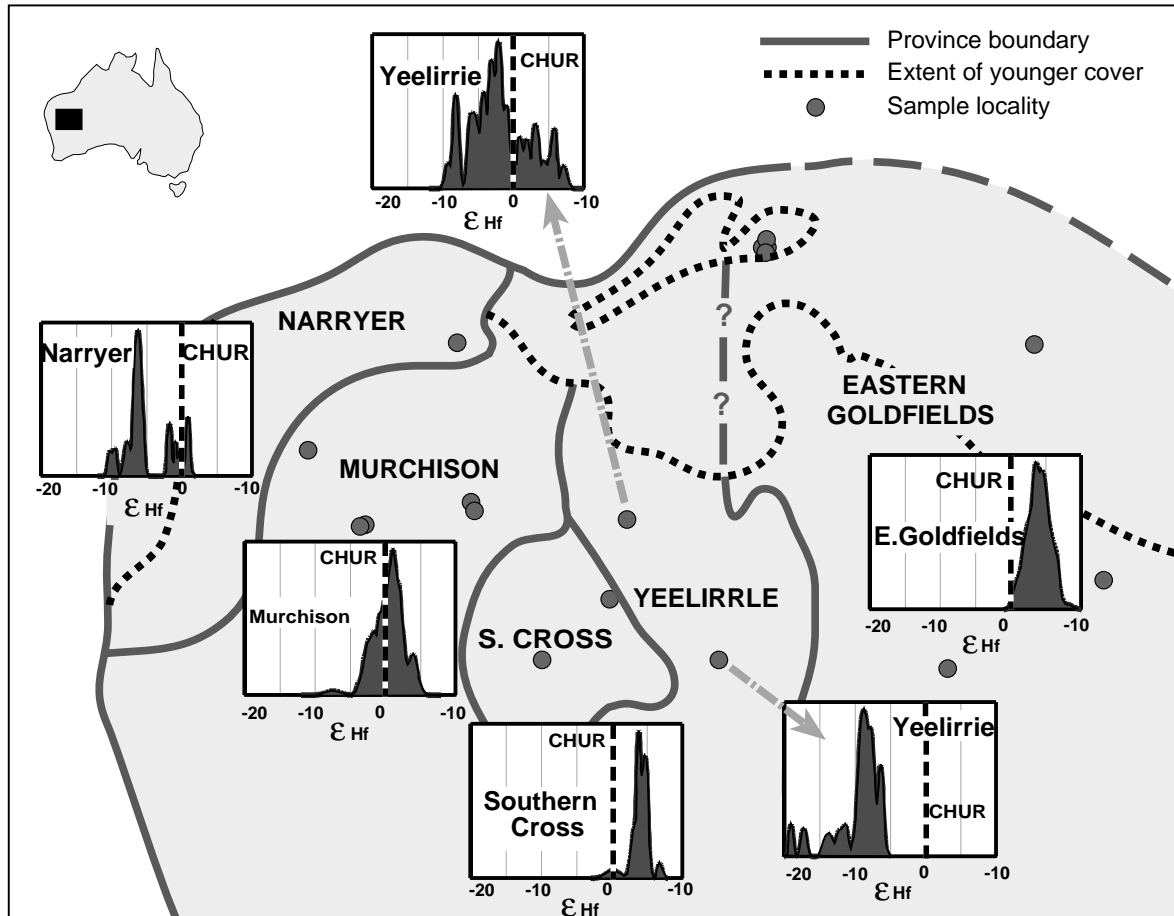


Fig. 8. Relative probability of ε_{Hf} data for zircons with ages of 2.6–2.8 Ga from each area, illustrating the juvenile character ($\varepsilon_{\text{Hf}} > 0$) of the magmatism in the Eastern Goldfields Province (including the Marymia Inlier) and the Southern Cross domain, and the major contribution of ancient crust ($\varepsilon_{\text{Hf}} = 0$) in the Yeelirrie and Narryer domains.

recorded in the Marymia Inlier, but the Hf-isotope data in the two areas are quite distinct.

The Hf-isotope data for the 2.6–2.8 Ga magmatism are summarised in Fig. 8. In the Eastern Goldfields Province (including the Marymia Inlier) and the Southern Cross domain, magmas of this age were derived from the Depleted Mantle reservoir, or from material with a short crustal residence time (<200 Ma). Champion and Sheraton (1997) found a gradient in ε_{Nd} in low-Cagranites across this province, suggesting the presence of older crust at depth in the west. However, this older crust is considered to thin to the north (D. Champion, personal communication), which would be consistent with the absence of an older

crustal signature, and the lack of any obvious variation in ε_{Hf} across the province, in our Hf-isotope data.

In the southern part of the Yeelirrie domain, the 2.6–2.8 Ga magmas appear to be derived entirely from older crust, dating back to ca. 3.7 Ga; no input from the Depleted Mantle reservoir is obvious. In the northern part of the domain, a similar crustal source is implied, but some rocks have high ε_{Hf} , and the range in ε_{Hf} suggests more mixing between the crustal and Depleted Mantle reservoirs. The data from the Murchison Province also suggest mixing between older crustal material and the reservoir. The Depleted Mantle contribution is most apparent in the eastern and central parts of the province (Belele and Cue map sheets).

In the west (*Byro* map sheet), the 2.6–2.8 Ga rocks may contain a Depleted Mantle contribution, but they also could be generated by melting of 3.2–3.4 Ga crust with range of Lu/Hf. In the Narryer Province, the isotope data do not require a Depleted Mantle source for the 2.6–2.8 Ga magmatism; all of the magmas could be generated from 3.4 to 3.5 Ga continental crust with a range of Lu/Hf corresponding to compositions between average crust and more mafic rock types.

The data summarised in Fig. 8 indicate a correlation between crustal age and the degree of crust–mantle interaction during the 2.6–2.8 Ga assembly of the craton. The domains with the oldest crust (Yeelirrie, Narryer) show the least evidence of mantle input during the widespread 2.6–2.8 Ga magmatism. This may reflect older and thicker lithosphere, which hindered mantle-derived magmas from getting through to high levels of the crust. However, it is likely that the Depleted Mantle signature, at least in felsic rocks, largely represents remelting of mafic rocks underplated on the crust shortly (<200 Ma) before. If so, the apparent low contribution from the Depleted Mantle source in the Yeelirrie and Narryer domains indicates that they had not experienced much underplating in the 2.9–3.2 Ga period. This difference underlines their suggested status as separate older domains (microcontinents).

These differences in the degree of crust–mantle interaction correlate with the style and intensity of mineralisation. Major gold deposits, in particular, are concentrated in the Eastern Goldfields Province, the Southern Cross domain, and the eastern edge of the Murchison Province, where young crust was remelted and juvenile contributions to the crust were most important in the craton amalgamation period (2.6–2.8 Ga). These correlations, if confirmed by more detailed analysis, may offer insights into the generation and localisation of large Archean gold deposits.

5.4. Younger magmas

There is a broad peak of zircon ages between 2.1 and 2.35 Ga, and this magmatism (or at least the zircons derived from it) is distributed widely across the craton. The zircons of this age classify as derived from a wide range of rock types, from felsic to mafic and

carbonatitic. The most significant concentration, in terms of numbers of zircons, is found in the Capricorn Orogen (*Mt. Egerton* map sheet), where this group includes zircons from both granitoids and possible carbonatites.

There is a distinct age peak at ca. 1.8 Ga, represented mainly by zircons from “low-Si granitoids” of the Capricorn Orogen. Scattered grains of this age are found in several samples from the northern edge of the craton, most notably in the Marymia Inlier. These early- to mid-Proterozoic magmatic rocks all have $\varepsilon_{\text{Hf}} < 0$, indicating that they are derived largely from older continental crust.

The remarkable cluster of ca. 540 Ma zircons in the NE part of the Eastern Goldfields Province (*Stanley* map sheet), because of its abundance and homogeneity, is interpreted as being of local derivation. If so, it represents a rejuvenation of the craton margin, involving metamorphism or remelting of the 2.75–3.0 Ga crust of the Eastern Goldfields Province. If these zircons are magmatic, their range in ε_{Hf} suggests mixing of crustal material with a large Depleted Mantle component. This magmatic, or more likely metamorphic, episode does not appear to have been recognised in outcrop, but the abundance of zircons with this signature suggests that it is volumetrically significant.

6. Conclusions

U–Pb and Hf-isotope analysis of >500 zircons from modern drainages across the northern part of the Yilgarn Craton and the adjacent Capricorn Orogen provides a broad view of crustal evolution in Archean and Proterozoic time. The oldest crustal components (3.7 Ga) are identified in the Yeelirrie geophysical domain that runs N–S down the middle of the craton; these components are represented by ancient zircons and also are reflected in the Hf model ages of younger magmas. This block of ancient crust does not appear to have been recognised previously, but it corresponds to a geophysically defined crustal domain (Whitaker, 2001), and seems to represent a significant element in the evolution of the craton. The Yeelirrie domain and the composite Narryer–Murchison block may thus represent ancient microcontinents, sandwiched with the juvenile terranes of the Southern Cross and Eastern Goldfields blocks.

There is no firm evidence for the existence of a Depleted Mantle reservoir beneath the Yilgarn Craton prior to 3.1–3.2 Ga, but this reservoir is a major contributor to crustal generation from 3.1 to 2.6 Ga; this suggests that much of the continental crust in the craton was generated after ca. 3.2 Ga. Magmatism from 1.8 to 2.3 Ga, associated with the Capricorn Orogeny, involved the recycling of older crust with no obvious contribution from the Depleted Mantle. However, a significant (and previously unrecognised?) 540 Ma episode in the NE part of the craton represents a reworking of the 2.7–3.0 Ga crust of the Eastern Goldfields Province.

This study demonstrates that the integrated application of U–Pb dating, Hf-isotope analysis and trace-element analysis to detrital zircon populations offers a rapid means of assessing the geochronology and crustal evolution history of different terranes, and gaining an overview of major trends in crustal evolution. By providing a broader framework for more detailed studies of individual rocks, it can point out gaps in our current knowledge of

the geology and geochronology of these areas, and indicate the most fruitful targets for such detailed work.

Acknowledgements

We thank Suzie Elhlou, Carol Lawson, and Ashwini Sharma for expert and cheerful assistance with the analytical work, Tom Bradley for preparation of many zircon grain mounts, and David Nelson, David Champion and Kevin Cassidy for useful discussions about Yilgarn magmatism. We are grateful to A. Whitaker for providing both a pre-publication copy of his new domain analysis, and guidance in its use. Useful reviews were contributed by R. Stern, J. Ketchum, M. Norman and an anonymous referee. This work was funded by two Small ARC grants and Macquarie University research funds. This is contribution no. 305 from the ARC National Key Centre for the Geochemical Evolution and Metallogeny of Continents (www.es.mq.edu.au/GEMOC/).

V8615-1	66.45	1.24	0.00	175	27	90	206	0.17604	0.00380	12.312	0.310	0.3135	0.0120	0.1389	0.0033	2622	36	2044
V8615-2	65.83	1.22	0.02	456	54	141	110	0.17915	0.00412	12.033	0.287	0.4870	0.0105	0.1393	0.0030	2645	38	2607
V8615-4	65.86	1.53	0.10	246	39	93	93	0.17659	0.00384	12.472	0.256	0.5119	0.0098	0.1394	0.0026	2621	36	2641
V8615-5	65.84	1.21	0.09	283	45	132	182	0.18034	0.00386	12.438	0.236	0.5001	0.0089	0.1425	0.0025	2656	36	2638
V8615-6	65.76	1.32	0.00	11	2	27	38	0.18087	0.00404	12.399	0.277	0.4968	0.0102	0.1376	0.0029	2661	36	2635
V8615-7	66.68	1.09	0.05	170	26	86	131	0.18868	0.00434	9.121	0.194	0.3507	0.0067	0.0898	0.0019	2731	38	2350
V8615-8	66.15	1.37	0.06	118	15	176	151	0.18124	0.00382	12.468	0.268	0.4986	0.0102	0.1389	0.0027	2664	34	2640
V8615-9	66.45	1.26	0.01	65	10	38	169	0.17977	0.00380	12.364	0.234	0.4983	0.0090	0.1470	0.0027	2651	34	2632
V8615-10	66.24	1.46	0.08	372	59	146	590	0.17900	0.00540	9.026	0.204	0.3630	0.0072	0.0999	0.0050	2644	50	2341
V8615-11	65.86	1.24	0.00	17	2	49	90	0.17829	0.00384	12.512	0.271	0.5086	0.0104	0.1374	0.0028	2637	36	2644
V8616-1	65.67	1.22	0.13	257	41	121	213	0.18021	0.00380	10.892	0.246	0.4381	0.0095	0.1386	0.0029	2655	34	2514
V8616-2	66.15	1.22	0.09	133	20	306	129	0.18247	0.00398	10.870	0.190	0.4316	0.0069	0.0708	0.0011	2675	36	2512
V8616-3	65.47	1.29	0.00	197	36	9	30	0.18276	0.00424	13.057	0.311	0.5178	0.0113	0.1389	0.0037	2678	38	2684
V8616-4	66.06	1.34	0.07	126	19	135	154	0.17748	0.00402	11.576	0.299	0.4732	0.0115	0.1269	0.0030	2629	38	2571
V8616-5	65.90	1.46	0.04	176	28	57	68	0.18109	0.00386	12.439	0.269	0.4978	0.0103	0.1377	0.0027	2663	36	2638
V8616-6	66.14	1.34	0.07	135	19	124	113	0.17999	0.00388	12.001	0.293	0.4834	0.0113	0.1302	0.0029	2653	36	2605
V8616-7	65.91	1.35	0.00	154	25	173	182	0.18463	0.00388	11.115	0.198	0.4363	0.0075	0.1411	0.0023	2695	34	2533
V8616-8	65.72	1.39	0.08	301	50	131	146	0.17761	0.00368	12.361	0.258	0.5044	0.0102	0.1076	0.0021	2631	34	2632
V8616-9	65.66	1.50	0.00	62	10	36	197	0.18082	0.00374	12.816	0.293	0.5141	0.0115	0.1287	0.0029	2660	34	2666
V8616-10	65.08	1.26	0.02	82	14	39	191	0.18044	0.00376	12.746	0.301	0.5124	0.0118	0.1331	0.0030	2657	34	2661
V8616-11	61.52	1.51	0.06	554	90	126	125	0.17987	0.00372	12.423	0.270	0.5009	0.0107	0.1368	0.0027	2652	34	2637
V8616-12	65.87	1.32	0.03	160	26	45	96	0.18136	0.00400	12.029	0.309	0.4815	0.0119	0.1306	0.0032	2665	36	2607

BE1769-19	66.71	1.46	0.06	221	35	28	65	0.05843	0.00242	0.716	0.030	0.0889	0.0021	0.0269	0.0009	546	90	548
BE1769-20	66.93	1.35	0.07	31	4	42	60	0.05748	0.00258	0.665	0.030	0.0839	0.0020	0.0252	0.0007	510	98	518
BE1769-21	65.49	1.29	0.10	216	36	28	62	0.21597	0.00442	16.916	0.370	0.5681	0.0127	0.1472	0.0033	2951	32	2930
BE1769-22	65.79	1.63	0.08	316	5	90	171	0.05751	0.00164	0.710	0.021	0.0895	0.0020	0.0268	0.0006	511	62	545
BE1769-23	67.31	0.93	0.04	167	26	34	71	0.04974	0.00286	0.368	0.021	0.0537	0.0013	0.0164	0.0006	183	132	318
BE1769-24	67.15	0.83	0.06	204	33	23	61	0.05766	0.00394	0.631	0.040	0.0792	0.0019	0.0246	0.0016	517	146	497
BE1769-25	66.19	1.25	0.09	230	40	3	8	0.19208	0.00600	13.466	0.421	0.5086	0.0131	0.1326	0.0056	2760	50	2713
BE1769-26	66.42	1.34	0.05	11	2	675	109	0.05880	0.00194	0.756	0.025	0.0932	0.0020	0.0290	0.0006	560	72	571
BE1769-27	67.12	0.91	0.26	923	114	287	135	0.05957	0.00254	0.825	0.032	0.0998	0.0018	0.0308	0.0011	588	92	611
BE1769-28	67.02	1.06	0.10	291	49	54	8	0.06061	0.00648	0.838	0.088	0.1004	0.0028	0.0317	0.0011	625	222	618
BE1769-29	66.81	1.06	0.07	82	12	331	30	0.05898	0.00330	0.742	0.041	0.0913	0.0022	0.0302	0.0007	566	120	564
BE1769-30	66.46	1.55	0.02	48	7	34	24	0.05815	0.00398	0.706	0.047	0.0881	0.0021	0.0291	0.0016	535	146	543
BE1769-31	66.81	1.48	0.14	430	74	18	9	0.19138	0.00490	13.761	0.334	0.5216	0.0110	0.1397	0.0041	2754	42	2733
BE1769-32	64.97	0.65	1.35	2933	306	2080	182	0.05707	0.00266	0.787	0.033	0.0993	0.0019	0.0323	0.0016	494	100	589
BE1769-33	66.15	1.18	0.03	38	5	164	37	0.05562	0.00450	0.657	0.051	0.0854	0.0018	0.0266	0.0013	437	176	513
BE1769-34	66.60	1.90	0.14	319	54	152	89	0.18928	0.00380	13.280	0.256	0.5090	0.0099	0.1430	0.0028	2736	32	2700
BE1769-35	66.41	1.29	0.01	55	8	61	35	0.05861	0.00238	0.707	0.027	0.0875	0.0017	0.0283	0.0008	553	88	543
BE1769-36	66.56	1.13	0.03	159	25	25	8	0.18757	0.00518	12.876	0.335	0.4980	0.0107	0.1376	0.0037	2721	46	2671
BE1769-37	65.85	1.52	0.22	886	138	567	276	0.07996	0.00160	2.189	0.041	0.1986	0.0037	0.0620	0.0011	1196	40	1178
BE1769-38	66.45	1.18	0.14	547	68	117	61	0.05381	0.00238	0.387	0.017	0.0521	0.0011	0.0167	0.0005	363	98	332
BE1769-39	66.69	1.42	0.04	55	7	258	87	0.05600	0.00258	0.697	0.029	0.0899	0.0017	0.0280	0.0009	452	102	537

BA3524-15	67.44	1.29	0.04	291	52	38	72	0.19932	0.00434	14.678	0.294	0.5340	0.0100	0.1244	0.0025	2821	36	2795
BA3524-16	66.64	1.12	0.13	300	53	11	34	0.18738	0.00488	13.947	0.331	0.5410	0.0107	0.1455	0.0043	2719	42	2746
BA3524-17	66.38	1.45	0.07	283	52	14	37	0.19159	0.00532	14.168	0.374	0.5369	0.0115	0.1467	0.0045	2756	46	2761
BA3524-18	66.77	1.11	0.11	238	41	10	30	0.18914	0.00566	14.018	0.393	0.5393	0.0117	0.1450	0.0052	2735	48	2751
BA3524-19	65.41	1.18	0.10	332	56	24	56	0.18649	0.00480	13.610	0.353	0.5288	0.0118	0.1446	0.0040	2711	42	2723
BA3524-20	66.19	1.42	0.16	537	81	46	57	0.18901	0.00462	13.753	0.332	0.5273	0.0111	0.1436	0.0033	2734	40	2733
BA3524-21	66.51	1.20	0.08	322	49	27	32	0.18954	0.00496	14.056	0.362	0.5375	0.0117	0.1480	0.0036	2738	42	2754
BA3524-21A					19	20	0.18724	0.00428	13.315	0.322	0.5158	0.0118	0.1107	0.0026	2718	38	2702	
BA3524-23	65.66	1.21	0.14	283	43	18	26	0.19771	0.00500	13.373	0.338	0.4905	0.0108	0.0983	0.0026	2807	42	2706
BA3524-24	67.04	1.18	0.13	491	78	23	65	0.19256	0.00448	14.094	0.337	0.5306	0.0115	0.1300	0.0033	2764	38	2756
BA3524-25	66.44	1.32	0.17	199	34	44	43	0.19070	0.00522	13.851	0.401	0.5268	0.0129	0.1310	0.0035	2748	44	2740
BA3524-26	66.37	1.04	0.07	217	34	18	35	0.18951	0.00442	13.765	0.318	0.5268	0.0111	0.1403	0.0033	2738	38	2734
BA3524-27	60.89	1.30	0.67	1363	142	220	134	0.19109	0.00440	13.697	0.275	0.5209	0.0090	0.0368	0.0007	2752	38	2729
BA3524-28	66.61	1.21	0.12	345	54	27	26	0.18655	0.00516	13.312	0.389	0.5179	0.0128	0.1276	0.0035	2712	46	2702
BA3524-30	66.68	1.32	0.12	354	56	127	83	0.19662	0.00642	12.829	0.434	0.4737	0.0125	0.0570	0.0018	2798	52	2667
BA3524-31	65.52	1.60	0.03	104	18	36	77	0.18231	0.00444	13.084	0.373	0.5226	0.0139	0.0542	0.0021	2674	40	2686
BA3524-32	66.28	1.13	0.00	173	27	19	29	0.18389	0.00404	13.096	0.310	0.5163	0.0118	0.1152	0.0027	2688	36	2687
BA3524-33	66.66	1.20	0.09	213	38	11	24	0.19088	0.00480	13.951	0.360	0.5298	0.0122	0.1253	0.0037	2750	42	2746
BA3524-34	66.91	1.26	0.02	272	45	24	26	0.18923	0.00436	13.156	0.300	0.5052	0.0107	0.1354	0.0030	2735	38	2691
BA3524-35	66.52	1.37	0.03	229	37	18	66	0.18462	0.00378	13.101	0.287	0.5148	0.0113	0.1247	0.0029	2695	34	2687
BA3524-36	66.75	1.15	0.11	250	41	10	21	0.18607	0.00526	13.260	0.417	0.5156	0.0143	0.1389	0.0050	2708	46	2698

BJ1824-10	66.10	1.39	0.01	6450	256	0.19512	0.00370	11.522	0.239	0.4212	0.0095	0.0189	0.0004	2786	30	2550		
BJ1824-11	60.05	1.00	0.99	825	97	245	95	0.18230	0.00376	12.579	0.293	0.5008	0.0119	0.1380	0.0034	2674	34	2649
BJ1824-12	66.53	1.05	0.08	162	24	512	139	0.18002	0.00340	11.983	0.221	0.4830	0.0095	0.1350	0.0025	2653	32	2603
BJ1824-13	66.54	1.10	0.09	206	31	355	83	0.18036	0.00344	12.545	0.253	0.5047	0.0108	0.1409	0.0029	2656	32	2646
BJ1824-14	66.66	1.05	0.05	242	37	316	87	0.18007	0.00432	12.300	0.323	0.4954	0.0125	0.1337	0.0048	2654	40	2628
BJ1824-15	67.14	1.13	0.04	257	39	387	93	0.18061	0.00342	12.096	0.233	0.4860	0.0099	0.1265	0.0025	2658	32	2612
BJ1824-16	65.48	1.04	0.12	232	34	298	110	0.18217	0.00344	12.886	0.245	0.5133	0.0104	0.1414	0.0027	2673	32	2671
BJ1824-17	66.31	1.14	0.05	125	19	337	93	0.18025	0.00342	12.533	0.248	0.5045	0.0106	0.1425	0.0029	2655	32	2645
BJ1824-18	67.04	1.36	0.00	293	39	927	103	0.18612	0.00354	13.182	0.273	0.5139	0.0113	0.0436	0.0009	2708	32	2693
BJ1824-19	66.76	1.18	0.06	258	39	355	82	0.18040	0.00344	12.092	0.240	0.4864	0.0103	0.1340	0.0027	2657	32	2612
BJ1824-20	66.14	1.14	0.03	31	4	17	15	0.12778	0.00302	6.469	0.155	0.3674	0.0080	0.1043	0.0030	2068	42	2042
BJ1824-21	66.28	1.10	0.01	180	28	153	48	0.18150	0.00346	12.584	0.240	0.5030	0.0102	0.1319	0.0026	2667	32	2649
BJ1824-22	67.32	1.32	0.08	160	24	185	52	0.18082	0.00358	12.237	0.256	0.4910	0.0107	0.1342	0.0027	2660	32	2623
BJ1824-23	66.87	1.08	0.07	274	42	310	104	0.18081	0.00348	12.410	0.261	0.4979	0.0111	0.1439	0.0030	2660	32	2636
BJ1824-24C	66.49	1.07	0.05		1203	167	0.21186	0.00408	8.818	0.180	0.3020	0.0065	0.0503	0.0010	2920	30	2319	
BJ1824-24R				167	30	224	88	0.18102	0.00346	11.687	0.233	0.4683	0.0099	0.1164	0.0023	2662	32	2580
BJ1824-25	66.11	1.21	0.07	146	23	210	56	0.18153	0.00456	12.008	0.320	0.4799	0.0118	0.1290	0.0034	2667	42	2605
BJ1824-26	66.55	0.97	0.01	72	12	223	68	0.18255	0.00350	11.765	0.233	0.4675	0.0098	0.1035	0.0020	2676	32	2586
BJ1824-27	66.68	1.16	0.08	183	31	61	22	0.25431	0.00578	21.925	0.539	0.6257	0.0153	0.2835	0.0068	3212	36	3180
BJ1824-28	66.38	1.13	0.08		162	59	0.18254	0.00350	12.466	0.249	0.4954	0.0105	0.1401	0.0028	2676	32	2640	
BJ1824-29	66.83	1.10	0.04		210	68	0.18456	0.00398	12.251	0.290	0.4815	0.0115	0.1349	0.0031	2694	36	2624	
BJ1824-30	66.48	1.33	0.07		127	48	0.18306	0.00370	11.739	0.248	0.4652	0.0101	0.1276	0.0027	2681	34	2584	

BU0701-10	61.28	1.38	0.24	407	60	118	1558	0.11493	0.00232	4.655	0.094	0.2917	0.0059	0.0834	0.0025	1879	26	1759
BU0701-12	64.67	1.54	0.10	763	115	614	1210	0.08855	0.00188	1.641	0.036	0.1334	0.0028	0.0394	0.0009	1394	37	986
BU0701-13	65.09	1.76	0.19	1118	154	300	212	0.18569	0.00378	12.965	0.253	0.5061	0.0097	0.0510	0.0010	2704	34	2677
BU0701-14	55.65	1.29	0.98	2967	328	8474	456	0.26946	0.00552	11.063	0.223	0.2975	0.0059	0.0044	0.0001	3303	32	2528
BU0701-16	66.68	1.42	0.00	287	44	45	82	0.18511	0.00392	12.763	0.234	0.5004	0.0088	0.0922	0.0018	2699	34	2662
BU0701-17	60.74	1.32	1.38	1132	137	112	317	0.14582	0.00496	4.419	0.120	0.2132	0.0044	0.0598	0.0038	2297	58	1716
BU0701-18	66.22	1.62	0.06	1359	145	3883	221	0.28275	0.00578	16.279	0.314	0.4174	0.0080	0.0067	0.0001	3378	32	2893
BU0701-19	64.83	1.43	0.24	1618	232	145	430	0.17438	0.00354	11.734	0.234	0.4878	0.0096	0.1340	0.0026	2600	34	2583
BU0701-21C	63.46	1.69	0.11	800	114	645	2806	0.16758	0.00334	7.869	0.149	0.3405	0.0065	0.0541	0.0010	2534	34	2216
BU0701-21R					41	659	0.12896	0.00260	6.643	0.123	0.3739	0.0069	0.1809	0.0035	2084	36	2065	
BU0701-22	66.67	1.37	0.08	187	33	31	91	0.18218	0.00376	12.745	0.255	0.5075	0.0100	0.1357	0.0027	2673	34	2661
BU0701-23	65.12	1.42	0.15	797	110	243	1107	0.14214	0.00438	5.219	0.120	0.2638	0.0054	0.0742	0.0038	2253	52	1856
BU0701-24	65.78	1.63	0.13	1919	229	1031	1164	0.25777	0.00514	11.216	0.227	0.3158	0.0064	0.0333	0.0007	3233	32	2541
BU0701-25	65.38	1.42	0.04	465	67	92	589	0.14222	0.00546	4.107	0.130	0.1919	0.0041	0.0538	0.0089	2254	66	1656
BU0701-26	63.09	1.84	0.14	822	112	54	948	0.17164	0.00458	10.115	0.197	0.4221	0.0077	0.1154	0.0127	2574	44	2445
BU0701-27	63.36	1.63	0.33	1569	217	617	1869	0.17514	0.00350	12.150	0.256	0.5030	0.0107	0.1211	0.0025	2607	34	2616
BU0701-28	66.57	1.35	0.01	112	17	180	114	0.18384	0.00386	11.721	0.211	0.4636	0.0081	0.0352	0.0006	2688	34	2582
BU0701-29	66.83	1.20	0.05	227	38	47	99	0.18142	0.00378	12.909	0.271	0.5164	0.0106	0.1331	0.0028	2666	34	2673
BU0701-30	64.18	1.45	0.17	926	143	146	1120	0.12821	0.00390	4.951	0.110	0.2783	0.0058	0.0793	0.0046	2074	54	1811
BU0701-31	65.50	1.49	0.23	1377	151	177	233	0.23775	0.00478	14.518	0.255	0.4440	0.0078	0.0679	0.0012	3105	32	2784
BU0701-32	66.93	1.43	0.05	204	29	34	106	0.18825	0.00390	12.265	0.232	0.4737	0.0088	0.1481	0.0028	2727	34	2625

BM1790-1	65.011	1.584	0.191	544	76	426	103	0.18364	0.00390	10.782	0.230	0.4263	0.0088	0.1277	0.0025	2686	34	2505
BM1790-2	58.855	1.205	0.986	713	83	294	237	0.27391	0.00788	15.249	0.317	0.3986	0.0079	0.1056	0.0053	3329	44	2831
BM1790-3	65.612	1.435	0.038	125	20	183	52	0.18412	0.00396	12.136	0.228	0.4781	0.0085	0.1153	0.0021	2690	36	2615
BM1790-4	65.886	1.455	0.082	590	85	1633	544	0.12836	0.00464	3.575	0.107	0.1977	0.0040	0.0562	0.0027	2076	62	1544
BM1790-5	66.7	1.263	0.017	177	27	328	82	0.18405	0.00370	12.873	0.234	0.5073	0.0092	0.1381	0.0024	2690	34	2670
BM1790-6	67.168	1.259	0.03	79	11	109	17	0.18186	0.00398	12.427	0.249	0.4956	0.0094	0.1393	0.0025	2670	36	2637
BM1790-7	66.501	1.508	0.052	327	53	264	187	0.18326	0.00370	12.294	0.249	0.4867	0.0099	0.1459	0.0029	2683	34	2627
BM1790-9	66.353	1.584	0.133	1287	172	599	210	0.18535	0.00382	10.568	0.226	0.4137	0.0088	0.1136	0.0023	2701	34	2486
BM1790-10	66.37	1.381	0.101	339	52	278	95	0.18420	0.00372	12.886	0.231	0.5073	0.0091	0.1440	0.0025	2691	34	2671
BM1790-11	65.969	1.383	0	185	29	223	34	0.22289	0.00454	16.884	0.317	0.5492	0.0103	0.1557	0.0028	3002	32	2928
BM1790-12		0.012	359	83	0.18035	0.00360	12.445	0.236	0.5003	0.0096	0.1368	0.0025	2656	32	2639			
BM1790-14	66.101	1.387	0.095	413	63	573	108	0.18362	0.00364	12.787	0.231	0.5048	0.0093	0.1303	0.0023	2686	32	2664
BM1790-15	65.76	1.324	0.211	756	99	537	125	0.18290	0.00418	11.940	0.282	0.4733	0.0106	0.1280	0.0028	2679	38	2600
BM1790-17	65.927	1.141	0.236	290	45	108	30	0.18503	0.00470	11.875	0.306	0.4654	0.0107	0.1302	0.0031	2698	42	2595
BM1790-18R					788	76	0.26256	0.00540	22.843	0.393	0.6306	0.0108	0.0404	0.0007	3262	32	3220	
BM1790-19	65.844	1.456	0.011	645	94	344	201	0.30202	0.00588	28.047	0.482	0.6731	0.0119	0.1857	0.0032	3481	30	3421
BM1790-21	65.902	1.313	0.082	152	23	395	135	0.18115	0.00356	12.004	0.222	0.4804	0.0091	0.1342	0.0024	2663	32	2605
BM1790-22	59.094	1.097	0.289	873	96	383	81	0.17997	0.00394	12.100	0.283	0.4875	0.0111	0.0641	0.0015	2653	36	2612
BM1790-23	66.212	1.526	0.05	331	44	751	147	0.18866	0.00396	12.202	0.232	0.4687	0.0087	0.0949	0.0018	2731	34	2620
BM1790-24	66.082	1.317	0.022	123	21	225	37	0.18190	0.00366	12.368	0.234	0.4930	0.0094	0.1325	0.0024	2670	34	2633

BM1790-59	65.052	1.582	0.15	568	90	281	106	0.27028	0.00540	24.511	0.465	0.6578	0.0126	0.1625	0.0030	3308	32	3289
BU3132-1	67.009	0.955	0.12	221	32	426	74	0.17923	0.00364	12.328	0.237	0.4989	0.0096	0.1344	0.0024	2646	34	2630
BU3132-2	65.712	1.527	0.07	350	54	703	204	0.18465	0.00366	12.909	0.230	0.5071	0.0092	0.1344	0.0022	2695	32	2673
BU3132-3	66.38	1.434	0.13	348	54	444	156	0.26474	0.00520	23.714	0.421	0.6497	0.0118	0.1667	0.0028	3275	30	3257
Southern Cross Domain, Sandstone Sheet																		
BM2764-1	65.96	1.40	0.04	402	74	53	149	0.19717	0.00382	14.664	0.294	0.5396	0.0112	0.1481	0.0029	2803	32	2794
BM2764-2	65.76	1.09	0.05	235	46	58	124	0.19860	0.00396	14.609	0.277	0.5335	0.0103	0.1222	0.0023	2815	32	2790
BM2764-3	66.56	1.63	0.05	369	66	4	13	0.19836	0.00488	14.352	0.342	0.5248	0.0113	0.1419	0.0044	2813	40	2773
BM2764-4	66.31	1.27	0.04	450	85	29	98	0.19858	0.00388	14.800	0.305	0.5407	0.0115	0.1516	0.0031	2815	32	2802
BM2764-5	65.33	1.60	0.27	1146	207	70	89	0.19887	0.00390	14.665	0.303	0.5351	0.0115	0.1250	0.0025	2817	32	2794
BM2764-7	66.97	1.57	0.05	615	116	36	126	0.19762	0.00384	14.199	0.304	0.5213	0.0116	0.1372	0.0029	2807	32	2763
BM2764-8	66.59	1.28	0.04	152	31	20	67	0.19739	0.00390	14.429	0.313	0.5303	0.0119	0.1445	0.0032	2805	32	2778
BM2764-9	65.61	1.36	0.14	726	122	21	35	0.19903	0.00402	14.764	0.306	0.5380	0.0114	0.1507	0.0030	2818	32	2800
BM2764-10	65.76	1.49	0.02	350	64	20	65	0.20033	0.00398	14.138	0.281	0.5119	0.0105	0.1398	0.0029	2829	32	2759
BM2764-25	67.00	1.33	0.11	465	72	23	82	0.19802	0.00386	14.041	0.307	0.5146	0.0118	0.1384	0.0030	2810	32	2752
BM2764-27	66.74	1.54	0.04	428	73	7	17	0.19527	0.00454	13.869	0.317	0.5153	0.0111	0.1403	0.0035	2787	38	2741
BM2764-28	65.33	1.34	0.20	865	140	14	26	0.20138	0.00460	12.889	0.284	0.4644	0.0097	0.1295	0.0029	2837	38	2672
BM2764-29	65.98	1.27	0.17	632	110	26	40	0.20136	0.00426	14.136	0.296	0.5093	0.0106	0.1377	0.0028	2837	34	2759
BM2764-30	66.12	1.14	0.13	373	65	22	24	0.19651	0.00396	14.124	0.305	0.5215	0.0116	0.1420	0.0029	2797	32	2758
BQ4356-1	65.02	1.28	0.29	682	111	89	168	0.19958	0.00378	14.333	0.304	0.5212	0.0118	0.1421	0.0029	2823	30	2772

BA1192-12	65.44	1.30	0.20	517	90	244	615	0.20247	0.00348	15.519	0.337	0.5559	0.0141	0.1464	0.0029	2846	28	2848
BA1192-13	64.57	1.75	0.17	330	54	156	2928	0.14602	0.00250	5.457	0.125	0.2711	0.0073	0.0887	0.0019	2300	30	1894
BA1192-15C	64.88	1.69	0.08	377	77	54	456	0.17669	0.00312	11.579	0.279	0.4759	0.0135	0.1510	0.0037	2622	30	2571
BA1192-15R						784	1878	0.11955	0.00450	4.205	0.115	0.2512	0.0065	0.0718	0.0036	1949	66	1675
BA1192-16	65.26	1.56	0.15	380	61	164	274	0.18341	0.00328	12.157	0.293	0.4813	0.0133	0.1221	0.0026	2684	30	2617
BA1192-17C	66.00	1.09	0.12	210	33	57	67	0.18206	0.00334	12.055	0.278	0.4806	0.0126	0.1325	0.0027	2672	30	2609
BA1192-17R						77	374	0.18082	0.00318	11.843	0.250	0.4758	0.0116	0.1300	0.0025	2660	30	2592
BA1192-18	65.33	1.38	0.22	1182	155	295	545	0.19866	0.00742	9.920	0.254	0.3614	0.0098	0.0987	0.0042	2815	60	2427
BA1192-20	65.52	1.41	0.01	340	45	147	231	0.19419	0.00344	12.256	0.286	0.4581	0.0123	0.1013	0.0021	2778	28	2624
BA1192-21C	66.30	1.13	0.00	146	22	83	46	0.18926	0.00392	10.155	0.250	0.3892	0.0103	0.0582	0.0013	2736	34	2449
BA1192-21R						835	885	0.19132	0.00338	8.342	0.197	0.3172	0.0087	0.0258	0.0005	2754	28	2269
BA1192-22	66.36	1.06	0.13	484	81	403	373	0.18552	0.00328	12.419	0.296	0.4861	0.0133	0.1285	0.0027	2703	30	2637
BA1192-23	66.54	1.61	0.11	829	115	144	409	0.18718	0.00330	12.159	0.289	0.4716	0.0129	0.1281	0.0027	2718	28	2617
BA1192-26	66.41	1.34	0.05	579	91	151	444	0.19189	0.00334	12.601	0.267	0.4771	0.0117	0.1418	0.0027	2758	28	2650
BA1192-27	64.95	1.33	0.00	630	91	156	128	0.18447	0.00338	11.839	0.243	0.4657	0.0107	0.1297	0.0024	2693	30	2592
BA1192-28	65.40	1.43	0.02	3203	516	558	828	0.21231	0.00384	7.978	0.188	0.2728	0.0073	0.0685	0.0015	2923	30	2229
BA1202-1R						20	115	0.18111	0.00596	8.499	0.194	0.3375	0.0080	0.0932	0.0068	2663	54	2286
BA1202-2	66.34	1.41	0.13	632	106	297	260	0.18139	0.00322	11.878	0.248	0.4752	0.0113	0.1350	0.0025	2666	30	2595
BA1202-4C	66.83	1.47	0.03	218	36	161	327	0.18576	0.00324	12.583	0.258	0.4920	0.0116	0.1283	0.0024	2705	28	2649
BA1202-4R						76	96	0.18536	0.00352	12.503	0.273	0.4896	0.0119	0.1108	0.0022	2701	32	2643
BA1202-5	66.21	1.45	0.10	281	48	212	349	0.17977	0.00690	9.427	0.256	0.3757	0.0102	0.1035	0.0047	2651	62	2380

BQ1125-7	65.88	1.11	0.05	208	35	186	208	0.18871	0.00394	13.867	0.348	0.5330	0.0132	0.0747	0.0018	2731	34	2741
BQ1125-8	65.47	1.24	0.14	507	80	191	205	0.18596	0.00370	13.138	0.318	0.5117	0.0126	0.1197	0.0027	2707	32	2690
BQ1125-9	66.32	1.16	0.06	330	52	638	274	0.18473	0.00368	10.178	0.234	0.3992	0.0094	0.0673	0.0014	2696	32	2451
BQ1125-10	65.97	1.47	0.05	367	58	221	208	0.18397	0.00364	13.364	0.317	0.5262	0.0128	0.1429	0.0032	2689	32	2706
BQ1125-12	66.42	1.30	0.09	448	67	412	407	0.18843	0.00390	13.415	0.294	0.5179	0.0111	0.0973	0.0019	2729	34	2709
BQ1125-13	65.83	1.49	0.05	309	47	174	298	0.19302	0.00406	14.275	0.352	0.5375	0.0128	0.1493	0.0034	2768	34	2768
BQ1125-14	67.04	1.18	0.06	210	29	188	113	0.19596	0.00458	8.636	0.236	0.3203	0.0081	0.0466	0.0012	2793	38	2300
BQ1125-15	50.25	3.04	2.32	1212	209	498	1396	0.15229	0.00456	7.152	0.165	0.3380	0.0065	0.0946	0.0037	2372	50	2131
BQ1125-16	66.22	1.30	0.00	215	34	74	62	0.18653	0.00410	12.607	0.283	0.4908	0.0103	0.1441	0.0029	2712	36	2651
BQ1125-18C	65.70	1.25	0.08	227	36	210	212	0.19255	0.00416	13.600	0.341	0.5126	0.0122	0.1406	0.0032	2764	36	2722
BQ1125-18R						186	562	0.20325	0.00426	12.153	0.300	0.4345	0.0103	0.1421	0.0032	2852	34	2616
BQ1125-19	66.05	1.53	0.09	2506	27516	699	657	0.20436	0.00428	12.581	0.241	0.4468	0.0082	0.0978	0.0017	2861	34	2649
BQ1125-20	58.37	4.54	1.02	8892	1274	760	7581	0.17120	0.00358	10.513	0.200	0.4456	0.0081	1.1612	0.0197	2569	34	2481
BQ1125-21	65.43	1.81	0.04	1060	204	1822	2111	0.15823	0.00332	5.476	0.109	0.2511	0.0048	0.0362	0.0007	2437	36	1897
BQ1125-22	66.04	1.02	0.02	156	26	46	119	0.19050	0.00416	13.424	0.302	0.5113	0.0108	0.1331	0.0029	2746	36	2710
BQ1125-23C	65.84	1.04	0.06	429	64	366	134	0.21736	0.00546	12.665	0.357	0.4227	0.0105	0.0258	0.0007	2961	40	2655
BQ1125-23R						117	91	0.22611	0.00502	14.276	0.330	0.4580	0.0099	0.0833	0.0018	3025	36	2768
BQ1125-24	65.93	1.39	0.04	232	35	89	98	0.19541	0.00430	14.400	0.295	0.5345	0.0101	0.1343	0.0025	2788	36	2776
BQ1125-25	65.93	1.45	0.17	373	59	137	124	0.19042	0.00410	13.536	0.301	0.5156	0.0108	0.1415	0.0029	2746	36	2718
BQ1125-26R						168	504	0.18594	0.00624	10.445	0.271	0.3970	0.0085	0.1087	0.0061	2707	54	2475
BQ1125-29	63.73	2.13	0.06	1290	233	639	881	0.17831	0.00370	7.764	0.163	0.3162	0.0064	0.0548	0.0010	2637	34	2204

BQ1134-2	66.65	1.41	0.15	316	49	105	110	0.17863	0.00348	12.434	0.231	0.5067	0.0099	0.1304	0.0023	2640	32	2638
BQ1134-3	65.51	1.46	0.08	302	50	372	217	0.16997	0.00322	10.665	0.223	0.4587	0.0105	0.0524	0.0010	2557	32	2494
BQ1134-4	66.04	1.38	0.00	141	23	105	138	0.18089	0.00348	12.033	0.235	0.4851	0.0100	0.1239	0.0023	2661	32	2607
BQ1134-5	66.19	1.43	0.06	144	24	115	97	0.18897	0.00390	13.660	0.280	0.5245	0.0106	0.0747	0.0014	2733	34	2726
BQ1134-6	67.03	1.28	0.04	220	38	59	64	0.18778	0.00422	13.648	0.291	0.5272	0.0104	0.0959	0.0020	2723	36	2726
BQ1134-7	66.83	1.24	0.07	667	113	216	105	0.18615	0.00382	13.349	0.290	0.5203	0.0113	0.0810	0.0016	2708	34	2705
BQ1134-8	65.17	1.41	0.08	227	38	66	60	0.18700	0.00388	13.513	0.285	0.5243	0.0109	0.1310	0.0026	2716	34	2716
BQ1134-9	66.08	1.31	0.12	263	45	95	83	0.18587	0.00416	13.406	0.290	0.5230	0.0106	0.1427	0.0028	2706	36	2709
BQ1134-10	65.82	1.47	0.05	125	22	174	131	0.18962	0.00378	13.761	0.293	0.5265	0.0114	0.0844	0.0017	2739	32	2733
BQ1134-11	65.81	1.26	0.11	177	29	94	60	0.18559	0.00386	13.053	0.302	0.5102	0.0117	0.1387	0.0030	2703	34	2683
BQ1134-12	66.72	1.34	0.16	432	71	604	769	0.18002	0.00356	10.514	0.211	0.4236	0.0086	0.0177	0.0003	2653	32	2481
BQ1134-13	67.08	1.38	0.05	497	92	174	130	0.18881	0.00380	13.572	0.292	0.5216	0.0113	0.1194	0.0024	2732	32	2720
BQ1134-14	65.48	1.32	0.14	308	54	108	83	0.18586	0.00382	13.367	0.276	0.5217	0.0107	0.0906	0.0018	2706	34	2706
BQ1134-15	66.59	1.42	0.20	370	59	148	91	0.18460	0.00378	12.724	0.299	0.5000	0.0118	0.1309	0.0029	2695	34	2659
BQ1134-16	66.66	1.22	0.04	253	43	109	142	0.18922	0.00390	13.793	0.337	0.5291	0.0130	0.0965	0.0023	2735	34	2736
Murchison Province, Byro Sheet																		
BG7784-3	63.29	1.37	0.33	1145	150	12042	263	0.20904	0.00442	10.093	0.178	0.3516	0.0059	0.0039	0.0001	2898	34	2443
BG7784-5	63.29	1.77	0.17	838	122	887	1228	0.15667	0.00450	5.807	0.124	0.2668	0.0051	0.0743	0.0041	2420	48	1947
BG7784-9	66.11	1.32	0.14	478	73	749	321	0.22700	0.00470	18.257	0.356	0.5844	0.0111	0.1621	0.0032	3031	32	3003
BG7784-10	65.44	1.37	0.02	586	85	9815	533	0.20813	0.00434	7.935	0.159	0.2768	0.0054	0.0098	0.0002	2891	34	2224
BG7784-11	65.59	1.36	0.20	944	129	508	142	0.18893	0.00392	13.259	0.233	0.5100	0.0087	0.0901	0.0016	2733	34	2698

BG7784-46	65.51	1.23	0.13	309	47	107	28	0.22214	0.00484	17.405	0.343	0.5690	0.0106	0.1596	0.0031	2996	34	2957
BG7784-47	57.63	1.31	1.36	2535	303	446	109	0.21661	0.00452	15.504	0.275	0.5196	0.0089	0.0805	0.0014	2956	34	2847
BG7784-48	60.79	1.25	0.54	1240	158	5782	286	0.20594	0.00424	9.845	0.171	0.3471	0.0059	0.0094	0.0002	2874	34	2420
BG7784-50	66.38	1.12	0.04	241	39	156	29	0.19033	0.00408	13.424	0.259	0.5123	0.0094	0.1371	0.0025	2745	36	2710
BG7784-51	66.71	1.74	0.01	229	38	104	200	0.19488	0.00396	13.150	0.254	0.4908	0.0094	0.0617	0.0013	2784	34	2690
BG7784-53	67.11	1.61	0.14	809	117	926	803	0.19095	0.00384	12.712	0.257	0.4851	0.0099	0.1442	0.0029	2750	32	2659
BG7784-54	65.80	1.35	0.13	693	103	401	218	0.21729	0.00454	13.624	0.283	0.4549	0.0092	0.1156	0.0024	2961	34	2724
BG7784-55	64.88	1.53	0.28	989	120	2898	504	0.19110	0.00390	13.731	0.238	0.5210	0.0088	0.0174	0.0003	2752	34	2731
BG7784-56	66.06	1.10	0	869	114	7818	524	0.23715	0.00484	10.350	0.185	0.3164	0.0055	0.0137	0.0002	3101	32	2467
BG7784-57	66.61	1.59	0.054	1015	116	8310	215	0.23602	0.00482	13.674	0.243	0.4200	0.0073	0.0070	0.0001	3093	32	2727
BG7784-58	64.93	1.47	0.174	1134	164	1645	1189	0.18047	0.00366	8.987	0.183	0.3612	0.0073	0.1032	0.0021	2657	34	2337
BG7784-59	65.74	1.45	0.115	686	105	683	665	0.19113	0.00384	13.637	0.261	0.5173	0.0099	0.1431	0.0027	2752	32	2725
BG7784-60	66.35	1.60	0.055	259	48	298	74	0.22243	0.00460	17.665	0.357	0.5759	0.0114	0.0487	0.0010	2998	34	2972
BG7784-61	64.72	1.41	0.071	201	30	47	301	0.19306	0.00386	13.977	0.249	0.5249	0.0094	0.1021	0.0021	2768	32	2748

Narryer Province, Robinson Range Sheet

BA1471-1	65.68	2.00	0.13	4471	605	1740	1688	0.14915	0.00296	4.483	0.076	0.2179	0.0037	0.0514	0.0009	2336	34	1728
BA1471-2	64.21	1.92	0.33	1145	189	861	338	0.19678	0.00392	12.330	0.204	0.4544	0.0076	0.0917	0.0016	2800	32	2630
BA1471-2R						255	617	0.16364	0.00372	9.132	0.150	0.4033	0.0063	0.1124	0.0070	2494	38	2351
BA1471-3	59.57	2.58	0.31	1526	214	1480	1603	0.14823	0.00292	5.263	0.089	0.2575	0.0044	0.0423	0.0008	2326	34	1863

BA1471-38C	65.48	1.71	0.15	740	102	1047	428	0.17760	0.00362	12.049	0.210	0.4929	0.0085	0.0803	0.0017	2631	34	2608
BA1471-38R						496	246	0.17927	0.00370	12.256	0.222	0.4967	0.0088	0.1484	0.0032	2646	34	2624
BA1471-39	64.98	2.27	0.13	5268	810	3486	1122	0.17049	0.00348	8.704	0.138	0.3708	0.0058	0.0178	0.0004	2562	34	2307
BA1471-40	66.25	1.28	0.06	838	124	1380	1153	0.17154	0.00442	9.649	0.188	0.4062	0.0069	0.1123	0.0056	2573	42	2402
BA1471-41	64.08	2.25	0.33	1809	246	432	764	0.17094	0.00346	9.588	0.139	0.4072	0.0058	0.0715	0.0013	2567	34	2396
BA1471-42	64.87	2.30	0.09	1815	283	313	1049	0.17139	0.00394	6.461	0.108	0.2715	0.0043	0.0748	0.0065	2571	38	2041
BA1471-43	64.44	3.27	0.05	1535	242	218	1885	0.13729	0.00300	4.865	0.077	0.2562	0.0039	0.0723	0.0110	2193	38	1796
BA1471-45	66.13	1.66	0.14	638	88	517	350	0.17779	0.00358	11.306	0.163	0.4617	0.0066	0.1360	0.0024	2632	34	2549
BA1471-46	63.84	3.26	0.09	3110	407	68290	3202	0.15205	0.00868	7.682	0.404	0.3151	0.0070	0.0870	0.0383	2369	96	2194
BA1471-47	66.16	1.43	0.14	242	37	326	231	0.18292	0.00370	12.229	0.188	0.4858	0.0074	0.1430	0.0027	2680	34	2622
BA1471-48	65.71	1.82	0.07	2516	339	1960	2898	0.11530	0.00300	4.059	0.084	0.2488	0.0039	0.0713	0.0053	1885	46	1646
BA1471-49	65.13	1.51	0.29	813	116	303	248	0.18098	0.00376	12.420	0.172	0.4978	0.0066	0.1583	0.0028	2662	34	2637
BA1471-50	63.48	2.27	0.21	1754	249	161	813	0.13830	0.00272	4.078	0.060	0.2126	0.0028	0.0594	0.0059	2206	34	1650
BA1471-52	65.20	2.06	0.089	781	112	141	521	0.18799	0.00384	12.303	0.227	0.4748	0.0086	0.1437	0.0033	2725	34	2628
BA1471-53	65.79	1.37	0.076	186	30	104	134	0.11183	0.00242	5.088	0.078	0.3299	0.0045	0.1017	0.0020	1829	38	1834
BA1471-55	65.40	1.48	0.185	490	73	629	221	0.17840	0.00362	12.221	0.187	0.4966	0.0075	0.1506	0.0027	2638	34	2622
BA1471-56	65.80	1.21	0.051	236	31	356	262	0.18206	0.00374	11.736	0.167	0.4675	0.0064	0.1323	0.0023	2672	34	2584
BA1471-57	63.76	1.96	0.132	700	106	727	1520	0.14947	0.00298	5.388	0.085	0.2614	0.0041	0.0401	0.0008	2340	34	1883
BA1471-58	65.92	1.65	0.138	991	150	716	1085	0.14725	0.00300	5.981	0.081	0.2947	0.0039	0.0741	0.0013	2314	34	1973
BA1471-59	64.76	1.87	0.128	3066	357	518	2755	0.11791	0.00280	3.403	0.061	0.2055	0.0032	0.0573	0.0074	1925	42	1505
BA1471-59R						327	1995	0.13531	0.00344	4.225	0.081	0.2207	0.0037	0.0609	0.0110	2168	44	1679

J8272-20	65.685	1.532	0.078	90	14	362	118	0.11001	0.00214	4.780	0.097	0.3153	0.0068	0.0932	0.0019	1800	36	1781
J8272-21	65.184	1.483	0.122	282	47	677	142	0.11035	0.00210	4.819	0.096	0.3169	0.0067	0.0940	0.0019	1805	34	1788
J8272-22	65.971	1.437	0.038	191	30	564	63	0.10992	0.00236	4.757	0.109	0.3140	0.0071	0.0970	0.0021	1798	38	1777
J8272-23	66.508	1.773	0.18	336	50	1139	161	0.10945	0.00216	4.738	0.104	0.3142	0.0073	0.0948	0.0021	1790	36	1774
J8272-24	63.883	1.581	0.26	207	32	342	105	0.10712	0.00386	4.418	0.131	0.2977	0.0062	0.0862	0.0032	1751	66	1716
J8272-25	65.889	1.745	0.03	65	8	189	443	0.13368	0.00246	7.138	0.132	0.3875	0.0078	0.1130	0.0022	2147	32	2129
J8272-26	65.036	1.573	0.08	399	52	404	342	0.10319	0.00380	3.511	0.099	0.2442	0.0058	0.0711	0.0041	1682	68	1530
J8272-27	66.578	1.729	0.04	103	16	254	99	0.14265	0.00280	7.394	0.126	0.3761	0.0066	0.1050	0.0018	2260	34	2160
J8272-28	64.366	1.387	0.22	270	42	354	233	0.14322	0.00268	7.783	0.131	0.3943	0.0071	0.0927	0.0016	2266	32	2206

V8615-2	27	2538	22	2600	22	0	0.281142	0.000353	0.011247	2.7	2.96	0.281125	3.26	2	S	Granitoid <65% SiO ₂
V8615-4	20	2665	20	2638	18	0	0.281128	0.000422	0.012959	2.82	2.96	0.281106	2.02	3	D	Granitoid <65% SiO ₂
V8615-5	18	2614	18	2692	18	0	0.281144	0.000611	0.018821	2.81	2.92	0.281112	3.06	3	OD	Granitoid <65% SiO ₂
V8615-6	22	2600	20	2606	22	0	0.281170	0.000021	0.000687	2.73	2.79	0.281169	5.21	3	N	Kimberlite
V8615-7	22	1938	20	1739	20	<0.05	0.281187	0.000385	0.012494	2.74	2.75	0.281166	6.80	2	O	Mafic rocks
V8615-8	22	2608	20	2629	20	0	0.281206	0.000182	0.006939	2.70	2.73	0.281196	6.26	4	DO	Carbonatite
V8615-9	18	2607	18	2771	18	0	0.281142	0.000125	0.004181	2.78	2.87	0.281135	3.78	4	O	Carbonatite
V8615-10	22	1997	20	1924	50	0.7	0.281102	0.000668	0.020486	2.87	3.03	0.281067	1.18	2	O	Granitoid <65% SiO ₂
V8615-11	22	2651	20	2602	20	0	0.281273	0.000030	0.001080	2.60	2.58	0.281271	8.28	5	N	Kimberlite
V8616-1	22	2342	22	2624	20	0	0.281199	0.000552	0.017024	2.73	2.79	0.281170	5.11	2	O	Granitoid <65% SiO ₂
V8616-2	18	2313	16	1383	16	<0.05	0.281207	0.000266	0.008739	2.70	2.73	0.281193	6.40	3	OD	Carbonatite
V8616-3	24	2690	22	2628	26	0	0.281129	0.000454	0.012272	2.82	2.92	0.281105	3.35	3	OD	Granitoid <65% SiO ₂
V8616-4	26	2497	24	2415	24	0	0.281198	0.000231	0.007590	2.71	2.78	0.281186	5.05	3	DO	Carbonatite
V8616-5	22	2604	20	2607	20	0	0.281198	0.000316	0.009726	2.72	2.76	0.281181	5.70	4	N	Granitoid <65% SiO ₂
V8616-6	24	2542	24	2474	22	0	0.281151	0.000235	0.008147	2.77	2.86	0.281139	3.94	4	OD	Carbonatite
V8616-7	18	2334	18	2668	16	0	0.281183	0.000299	0.009191	2.74	2.77	0.281167	5.96	4	O	Granitoid <65% SiO ₂
V8616-8	20	2633	20	2066	20	0	0.281179	0.000595	0.017469	2.76	2.86	0.281148	3.75	3	O	Granitoid <65% SiO ₂
V8616-9	22	2674	22	2447	22	0	0.281126	0.000107	0.003328	2.80	2.90	0.281120	3.46	3	L	Carbonatite
V8616-10	24	2667	24	2526	22	0	0.281219	0.000177	0.005225	2.68	2.70	0.281210	6.57	4	LO	Carbonatite
V8616-11	22	2618	22	2592	20	0	0.281193	0.000979	0.029573	2.77	2.86	0.281142	4.03	4	O	Granitoid 70–75% SiO ₂
V8616-12	26	2534	24	2480	24	0	0.281111	0.000324	0.009792	2.83	2.95	0.281094	2.64	4	O	Granitoid <65% SiO ₂
V8616-13	22	2633	20	2623	20	0	0.281143	0.000140	0.004741	2.78	2.86	0.281136	4.29	3	N	Carbonatite

BE1769-26	32	574	22	577	22	0.09	0.282012	24	0.000021	0.000651	1.64	2.35	0.282012	-14.14	5	N	Kimberlite
BE1769-27	38	613	18	614	36	0.7	0.282593	26	0.002059	0.081673	0.93	1.12	0.282570	6.25	5	N	Mafic rocks
BE1769-28	106	617	28	631	34	0	0.282485	24	0.000756	0.022138	1.04	1.31	0.282476	3.78	5	N	Mafic rocks
BE1769-29	54	563	24	601	24	0	0.281765	19	0.000183	0.006277	1.98	2.87	0.281763	-22.82	5	N	Carbonatite
BE1769-30	66	544	24	580	54	0	0.282568	15	0.000070	0.002495	0.91	1.16	0.282567	4.95	5	N	Carbonatite
BE1769-31	24	2706	22	2642	30	0	0.281138	18	0.000813	0.023337	2.83	2.89	0.281094	4.77	5	N	Granitoid <65% SiO ₂
BE1769-32	42	610	18	642	50	0.7	0.282582	54	0.007783	0.365432	1.12	1.32	0.282507	1.89	4	N	Mafic rocks
BE1769-33	78	528	22	530	48	0.4	0.281690	24	0.000074	0.002608	2.07	3.10	0.281689	-28.37	5	N	Carbonatite
BE1769-34	20	2652	20	2701	20	0	0.281094	14	0.000469	0.013487	2.86	2.96	0.281069	3.45	5	N	Granitoid <65% SiO ₂
BE1769-35	38	541	20	563	30	0	0.282304	20	0.000096	0.003417	1.26	1.73	0.282303	-3.99	5	N	Carbonatite
BE1769-36	26	2605	22	2606	26	0	0.281043	17	0.000368	0.011310	2.92	3.07	0.281023	1.47	5	N	Mafic rocks
BE1769-37	18	1168	18	1215	18	0	0.281835	17	0.001494	0.046905	1.95	2.41	0.281800	-6.97	5	N	Granitoid 70–75% SiO ₂
BE1769-38	44	327	22	334	32	0.16	0.282610	14	0.000950	0.037439	0.88	1.19	0.282603	2.29	5	N	Mafic rocks
BE1769-39	42	555	18	559	30	0.4	0.282510	19	0.000083	0.003123	0.99	1.34	0.282509	1.00	5	N	Carbonatite
BE1769-40	38	581	18	583	32	0.3	0.282220	17	0.001082	0.031949	1.41	1.94	0.282209	-7.81	5	N	Granitoid 70–75% SiO ₂
BE1769-41	36	2668	26	2664	50	0	0.281155	19	0.000921	0.028026	2.82	2.84	0.281104	5.94	5	N	Mafic rocks
BE1769-42	28	561	20	581	28	0.12	0.282487	16	0.000045	0.001963	1.02	1.34	0.282487	2.16	5	N	Carbonatite
BE1769-43R	20	2688	20	1435	22	0	0.281093	20	0.001254	0.047270	2.92	3.06	0.281025	1.66	5	ON	
BE1769-44	40	349	20	369	22	0.13	0.282587	18	0.000778	0.024604	0.91	1.26	0.282582	0.78	5	N	Mafic rocks
BE1769-45	156	581	34	571	122	0	0.282658	16	0.000042	0.001477	0.79	0.93	0.282658	9.43	5	N	Carbonatite
BE1769-46	20	548	18	577	24	0	0.281710	19	0.000528	0.016108	2.07	3.01	0.281704	-25.37	4	N	Granitoid <65% SiO ₂

BA3524-16	24	2788	20	2745	30	0	0.281114	32	0.000785	0.021618	2.86	2.96	0.281072	3.15	3	N	Mafic rocks
BA3524-17	26	2770	22	2766	30	0	0.281098	30	0.000584	0.015689	2.87	2.95	0.281066	3.84	3	N	Granitoid <65% SiO ₂
BA3524-18	28	2780	22	2737	36	0	0.281021	40	0.000600	0.017225	2.97	3.13	0.280988	0.57	4	N	Mafic rocks
BA3524-19	26	2737	22	2730	28	0	0.281123	24	0.000773	0.022614	2.85	2.95	0.281081	3.30	3	N	Mafic rocks
BA3524-20	24	2730	22	2711	22	0	0.281072	19	0.000939	0.030362	2.93	3.06	0.281021	1.71	3	N	Granitoid 70–75% SiO ₂
BA3524-21	26	2773	22	2790	24	0	0.281139	24	0.000675	0.021694	2.82	2.88	0.281102	4.70	3	N	Mafic rocks
BA3524-21A	24	2681	22	2121	24	0											
BA3524-23	26	2573	22	1894	26	0	0.281104	36	0.000580	0.018769	2.86	2.90	0.281072	5.27	4	N	Granitoid <65% SiO ₂
BA3524-24	24	2744	22	2469	26	0	0.281161	34	0.001087	0.033393	2.82	2.86	0.281101	5.29	3	O	Mafic rocks
BA3524-25	28	2728	24	2489	28	0	0.281074	30	0.000424	0.012125	2.89	2.99	0.281051	3.11	3	N	Granitoid <65% SiO ₂
BA3524-26	24	2728	20	2654	24	0	0.281152	28	0.000532	0.016766	2.79	2.84	0.281123	5.43	4	N	Mafic rocks
BA3524-27	20	2703	18	731	20	0	0.281084	32	0.001796	0.084569	2.98	3.13	0.280986	0.89	2	DO	Syenite
BA3524-28	30	2690	24	2427	28	0	0.281078	36	0.000726	0.022918	2.90	3.04	0.281039	1.82	3	N	Granitoid <65% SiO ₂
BA3524-30	34	2500	26	1121	32	0	0.281116	26	0.000692	0.021567	2.85	2.89	0.281078	5.26	3	N	Granitoid <65% SiO ₂
BA3524-31	28	2710	26	1067	38	0	0.281153	20	0.000180	0.005236	2.77	2.84	0.281143	4.62	3	O	Carbonatite
BA3524-32	24	2683	22	2203	24	0	0.281142	18	0.000396	0.012281	2.80	2.88	0.281121	4.15	4	N	Mafic rocks
BA3524-33	26	2741	24	2387	30	0	0.281167	28	0.000527	0.014340	2.77	2.79	0.281138	6.26	3	ON	Granitoid <65% SiO ₂
BA3524-34	22	2636	22	2567	22	0	0.281076	30	0.000590	0.017405	2.90	3.01	0.281044	2.55	4	N	Granitoid <65% SiO ₂
BA3524-35	22	2677	22	2374	24	0	0.281119	32	0.000439	0.013448	2.83	2.93	0.281096	3.42	4	ON	Granitoid <65% SiO ₂
BA3524-36	32	2680	28	2629	36	0	0.281154	24	0.000582	0.017533	2.79	2.86	0.281123	4.70	4	N	Mafic rocks
BA3524-37	20	2071	20	284	20	0	0.281061	22	0.000733	0.034676	2.93	3.30	0.281026	-6.50	4	M	Syenite
BA3524-38	26	2442	22	2312	30	<0.05	0.281062	16	0.000440	0.013418	2.90	3.00	0.281038	3.22	5	N	Granitoid <65% SiO ₂

BJ1824-19	20	2555	22	2542	20	0	0.281151	12	0.000540	0.017622	2.80	2.90	0.281123	3.47	4	N	Mafic rocks
BJ1824-20	24	2017	22	2005	30	0	0.281436	17	0.000056	0.002200	2.39	2.63	0.281434	0.48	4	ON	Carbonatite
BJ1824-21	20	2627	20	2505	20	0	0.281133	13	0.000410	0.013146	2.81	2.91	0.281111	3.31	4	N	Mafic rocks
BJ1824-22	20	2575	22	2545	20	0	0.281138	14	0.000302	0.009758	2.80	2.89	0.281122	3.52	4	O	Granitoid <65% SiO ₂
BJ1824-23	20	2605	22	2718	20	0	0.281172	13	0.000642	0.020477	2.78	2.86	0.281138	4.10	4	N	Mafic rocks
BJ1824-24C	20	1701	22	991	20	<0.05									2	O	Mafic rocks
BJ1824-24R	20	2476	22	2226	20	0	0.281174	15	0.000458	0.012614	2.76	2.83	0.281150	4.56			
BJ1824-25	26	2527	24	2453	26	0	0.281151	17	0.000315	0.009734	2.78	2.86	0.281134	4.13	4	N	Granitoid <65% SiO ₂
BJ1824-26	20	2473	20	1991	20	0	0.281149	16	0.000199	0.005961	2.77	2.85	0.281138	4.49	4	ON	Carbonatite
BJ1824-27	24	3132	24	5045	24	0	0.281162	17	0.000432	0.012679	2.77	2.46	0.281134	17.30	4	N	Mafic rocks
BJ1824-28	20	2594	22	2651	20	0									4	DO	
BJ1824-29	24	2534	24	2558	24	0									3	DN	
BJ1824-30	22	2463	22	2426	20	0									4	N	
BJ1824-31	20	2616	22	2633	20	0									4	D	
BJ1824-32	18	2368	20	345	18	0	0.281158	10	0.000276	0.009030	2.77	2.78	0.281143	6.41	3	ON	Carbonatite
BJ1824-33	22	2638	22	2613	22	0									4	N	
BJ1824-34	20	2626	22	2693	20	0									4	N	
BJ1824-35	20	2609	20	2640	18	0									4	N	
BJ1824-36	22	2608	22	2636	22	0									5	N	
BJ1824-37	20	2613	22	2644	22	0									5	ON	
BJ1824-38	22	2581	22	2168	22	0									3	ON	

BU0701-14	20	1679	20	88	18	<0.05	0.280535	26	0.004185	0.185705	3.96	4.32	0.280260	-11.66	4	OM	Granitoid >75% SiO ₂
BU0701-16	18	2616	18	1783	20	0	0.280808	24	0.000503	0.016229	3.24	3.61	0.280781	-7.67	4	OM	Granitoid <65% SiO ₂
BU0701-17	28	1246	20	1174	64	3	0.280806	15	0.001707	0.069171	3.34	4.00	0.280729	-19.14	3	DMO	Syenite
BU0701-18	20	2248	20	135	18	<0.05	0.280606	18	0.001472	0.067727	3.58	3.73	0.280507	-1.02	4	OM	Granitoid 70–75% SiO ₂
BU0701-19	20	2561	20	2541	20	0	0.280940	36	0.002670	0.091289	3.25	3.64	0.280803	-9.28	4	ONM	Granitoid 70–75% SiO ₂
BU0701-21C	18	1889	20	1066	18	<0.05	0.280552	18	0.001106	0.038188	3.62	4.34	0.280497	-21.75	4	DM	Granitoid 70–75% SiO ₂
BU0701-21R	18	2048	18	3360	20	0										Insufficient parameters	
BU0701-22	20	2646	20	2572	20	0	0.280770	26	0.000398	0.011025	3.28	3.70	0.280749	-9.44	3	ON	Granitoid <65% SiO ₂
BU0701-23	22	1509	20	1446	52	1.0	0.280813	18	0.001268	0.045090	3.29	3.97	0.280757	-19.19	2	MD	Granitoid 70–75% SiO ₂
BU0701-24	20	1769	20	662	20	<0.05	0.280593	12	0.002309	0.094915	3.68	3.97	0.280444	-6.77	4	MD	Granitoid 70–75% SiO ₂
BU0701-25	32	1132	22	1059	164	8.4	0.280766	22	0.000776	0.026372	3.31	4.02	0.280732	-20.06	3	O	Granitoid <65% SiO ₂
BU0701-26	20	2270	18	2206	110	1.2	0.280531	14	0.001005	0.036030	3.64	4.35	0.280480	-21.39	4	MD	Granitoid 70–75% SiO ₂
BU0701-27	22	2627	22	2310	20	0	0.280829	24	0.002185	0.077362	3.35	3.82	0.280716	-12.19	3	OD	Granitoid 70–75% SiO ₂
BU0701-28	18	2455	18	698	18	0	0.280791	24	0.000212	0.006665	3.23	3.62	0.280780	-7.99	4	ON	Carbonatite
BU0701-29	22	2684	20	2525	22	0	0.280805	34	0.000517	0.015170	3.24	3.64	0.280778	-8.59	3	O	Granitoid <65% SiO ₂
BU0701-30	22	1583	20	1542	58	0.6	0.280886	22	0.001621	0.051560	3.23	3.95	0.280820	-21.19	4	OM	Granitoid 70–75% SiO ₂
BU0701-31	18	2368	18	1328	18	<0.05	0.280494	17	0.001670	0.074456	3.75	4.18	0.280391	-11.78	4	OD	Granitoid 70–75% SiO ₂
BU0701-32	18	2500	18	2791	20	0	0.280780	26	0.000339	0.011519	3.26	3.64	0.280762	-7.69	4	DON	Granitoid <65% SiO ₂
BU0701-33	20	1859	18	1832	68	0.6	0.280613	34	0.001342	0.042937	3.56	4.49	0.280557	-29.81	3	DMN	Granitoid 70–75% SiO ₂
BU0701-34	22	1261	22	955	22	<0.05	0.280620	14	0.001590	0.050397	3.58	4.54	0.280557	-31.88	4	OM	Granitoid 70–75% SiO ₂
BU0701-35	22	3300	20	3479	20	0	0.280577	28	0.001120	0.035191	3.59	3.79	0.280503	-2.97	4	N	Granitoid 70–75% SiO ₂
BU0701-36	20	2664	20	2986	18	0	0.280921	19	0.001595	0.053809	3.18	3.51	0.280837	-6.32	4	OD	Granitoid 70–75% SiO ₂

BM1790-11	18	2822	18	2924	18	0	0.280609	17	0.000342	0.010748	3.48	3.82	0.280589	-7.23	2	N	Granitoid <65% SiO ₂
BM1790-12	18	2615	20	2591	18	0	0.281095	24	0.000250	0.007318	2.85	2.99	0.281082	1.99	2	N	Insufficient parameters
BM1790-14	18	2635	18	2475	18	0	0.280995	26	0.000750	0.023991	3.01	3.24	0.280955	-1.79	2	N	Granitoid <65% SiO ₂
BM1790-15	24	2498	22	2434	22	0	0.280989	17	0.001222	0.045942	3.06	3.32	0.280924	-3.06	3	N	Granitoid 70–75% SiO ₂
BM1790-17	26	2463	24	2474	24	0	0.280797	20	0.000644	0.020466	3.26	3.65	0.280763	-8.36	4	N	Mafic rocks
BM1790-18R	18	3152	18	800	18	0	0.280605	14	0.000816	0.034394	3.52	3.71	0.280552	-2.23	3	DO	
BM1790-19	18	3318	18	3442	18	0	0.280517	18	0.001063	0.035653	3.66	3.79	0.280443	-0.78	2	DO	Granitoid 70–75% SiO ₂
BM1790-21	18	2529	18	2545	18	0	0.280983	19	0.000294	0.009311	2.99	3.23	0.280968	-1.90	2	N	Granitoid <65% SiO ₂
BM1790-22	24	2560	22	1257	22	0	0.280953	15	0.001439	0.064064	3.12	3.44	0.280877	-5.35	3	ON	Mafic rocks
BM1790-23	18	2478	18	1832	18	0	0.281119	20	0.000469	0.017433	2.83	2.91	0.281094	4.22	4	DO	Granitoid <65% SiO ₂
BM1790-24	18	2584	20	2515	18	0	0.280972	22	0.000265	0.007496	3.01	3.25	0.280958	-2.08	3	N	Granitoid <65% SiO ₂
BM1790-25	18	2593	18	2631	18	0	0.280885	22	0.000698	0.021309	3.15	3.49	0.280848	-6.06	4	N	Granitoid <65% SiO ₂
BM1790-27	20	2570	20	2570	20	0	0.280997	17	0.000856	0.018181	3.02	3.27	0.280952	-2.51	3	N	Granitoid <65% SiO ₂
BM1790-28	20	2605	20	2359	18	0	0.280886	20	0.000407	0.013299	3.13	3.46	0.280864	-5.52	2	N	Granitoid <65% SiO ₂
BM1790-29	18	2591	20	2627	18	0	0.280982	24	0.000541	0.016309	3.01	3.26	0.280953	-2.36	4	N	Granitoid <65% SiO ₂
BM1790-32	18	2589	18	2838	18	0	0.280896	19	0.000714	0.022458	3.14	3.40	0.280857	-3.39	3	ON	Mafic rocks
BM1790-33	20	1778	20	74	22	<0.05	0.281079	18	0.001165	0.046057	2.94	3.03	0.281014	3.03	3	OD	Mafic rocks
BM1790-34	20	2706	18	1896	20	0	0.280915	22	0.000245	0.007660	3.08	3.32	0.280902	-2.21	2	ON	Granitoid <65% SiO ₂
BM1790-35	20	2379	20	779	20	0	0.281089	20	0.001481	0.053828	2.95	3.10	0.281009	0.92	3	N	Granitoid 70–75% SiO ₂
BM1790-36	18	2462	16	1094	18	0	0.281026	19	0.000266	0.008327	2.94	3.10	0.281012	0.85	3	N	Granitoid <65% SiO ₂
BM1790-37	22	2677	20	2637	20	0	0.280955	22	0.001267	0.048867	3.11	3.36	0.280886	-3.02	3	N	Granitoid 70–75% SiO ₂

Southern Cross Domain, Sandstone Sheet																	
BM2764-1	20	2782	20	2792	20	0	0.281062	10	0.000868	0.023201	2.94	3.03	0.281014	3.11	4	N	Granitoid <65% SiO ₂
BM2764-2	18	2756	20	2330	18	0	0.281060	12	0.000695	0.017436	2.93	3.00	0.281021	3.66	4	ON	Mafic rocks
BM2764-3	24	2719	22	2682	32	0	0.281093	12	0.000664	0.018154	2.88	2.93	0.281056	4.85	4	N	Granitoid <65% SiO ₂
BM2764-4	20	2786	22	2854	20	0	0.281081	13	0.001091	0.028440	2.93	3.01	0.281020	3.62	4	OD	Granitoid <65% SiO ₂
BM2764-5	20	2763	22	2381	20	0	0.281226	16	0.002121	0.057710	2.81	2.81	0.281108	6.78	4	LN	Granitoid 70–75% SiO ₂
BM2764-7	22	2704	22	2598	20	0	0.281067	20	0.001207	0.031502	2.96	3.06	0.281000	2.71	4	N	Granitoid 70–75% SiO ₂
BM2764-8	22	2743	22	2727	22	0	0.281056	12	0.000392	0.009581	2.91	2.98	0.281034	3.88	3	DN	Granitoid <65% SiO ₂
BM2764-9	20	2775	22	2836	20	0	0.281122	12	0.001475	0.042918	2.90	2.96	0.281040	4.39	4	N	Granitoid 70–75% SiO ₂
BM2764-10	20	2665	20	2644	20	0	0.281056	10	0.000710	0.018947	2.93	3.01	0.281016	3.82	4	O	Granitoid <65% SiO ₂
BM2764-25	22	2676	22	2620	22	0	0.280976	54	0.000893	0.028163	3.05	3.22	0.280926	0.16	4	O	Granitoid <65% SiO ₂
BM2764-27	22	2679	22	2653	26	0	0.281095	11	0.000777	0.022356	2.89	2.96	0.281052	4.09	4	N	Granitoid <65% SiO ₂
BM2764-28	22	2459	20	2460	22	0	0.281139	11	0.001718	0.051991	2.90	2.94	0.281042	4.94	4	N	Granitoid 70–75% SiO ₂
BM2764-29	20	2654	20	2607	20	0	0.281127	17	0.001418	0.040058	2.89	2.93	0.281047	5.12	4	N	Granitoid 70–75% SiO ₂
BM2764-30	22	2705	22	2684	20	0	0.281100	20	0.000933	0.026330	2.89	2.96	0.281048	4.19	4	N	Mafic rocks
BQ4356-1	22	2704	22	2685	20	0	0.281118	15	0.001434	0.043063	2.91	2.96	0.281038	4.44	3	OD	Granitoid 70–75% SiO ₂
BQ4356-2	20	2661	20	2609	18	0	0.281078	19	0.000695	0.020817	2.90	2.96	0.281039	4.42	3	N	Granitoid <65% SiO ₂
BQ4356-3	22	2639	22	2634	20	0	0.281127	13	0.001863	0.054180	2.93	3.00	0.281023	3.77	3	ON	Granitoid 70–75% SiO ₂
BQ4356-4	20	2540	22	2489	20	0	0.281131	11	0.001152	0.031275	2.87	2.92	0.281067	4.79	4	MN	Granitoid 70–75% SiO ₂
BQ4356-5	20	2724	20	2740	20	0	0.281185	18	0.002458	0.075429	2.89	2.95	0.281048	4.56	3	D	Mafic rocks
BQ4356-6	20	2705	22	2332	20	0	0.281286	16	0.003947	0.118034	2.87	2.91	0.281067	4.97	3	DN	Granitoid 70–75% SiO ₂

BA1192-22	24	2554	28	2443	22	0	0.281091	14	0.001255	0.036725	2.93	3.08	0.281024	1.06	3	DO	Mafic rocks
BA1192-23	24	2491	28	2436	22	0	0.281067	9	0.001179	0.041497	2.95	3.11	0.281004	0.70	3	DN	Granitoid 70–75% SiO ₂
BA1192-26	22	2515	24	2680	20	0	0.281089	14	0.001109	0.034798	2.92	3.03	0.281028	2.54	3	DO	Granitoid 70–75% SiO ₂
BA1192-27	20	2465	24	2466	18	0	0.281125	12	0.001124	0.038177	2.87	3.00	0.281065	2.29	4	LD	Insufficient parameters
BA1192-28	24	1555	26	1340	22	<0.05	0.281240	11	0.005915	0.179919	3.11	3.20	0.280897	1.83	3	OM	Granitoid 70–75% SiO ₂
BA1202-1R	22	1875	24	1801	72	0.8									3	MO	
BA1202-2	20	2506	24	2559	18	0	0.281075	19	0.001230	0.036017	2.95	3.14	0.281010	-0.32	5	N	Granitoid 70–75% SiO ₂
BA1202-4C	20	2579	24	2440	18	0	0.281064	15	0.000396	0.011927	2.90	3.04	0.281043	1.78	4	ODN	Granitoid <65% SiO ₂
BA1202-4R	22	2569	24	2125	20	0											
BA1202-5	28	2056	28	1990	46	1.2	0.281031	11	0.000538	0.015540	2.95	3.16	0.281003	-0.94	3	NO	Granitoid <65% SiO ₂
BA1202-6	24	1975	28	1790	20	<0.05	0.281046	11	0.000465	0.013588	2.93	3.12	0.281022	-0.20	4	DO	Granitoid <65% SiO ₂
BA1202-7	20	2523	20	2521	18	0	0.281054	15	0.000495	0.013881	2.92	3.08	0.281028	0.95	4	OD	Granitoid <65% SiO ₂
BA1202-8	20	2521	22	2520	20	0	0.281090	14	0.000724	0.020429	2.89	3.03	0.281051	1.68	4	ON	Granitoid <65% SiO ₂
BA1202-9	22	2374	24	2556	20	0	0.281050	11	0.000791	0.023387	2.95	3.10	0.281007	0.86	4	ON	Granitoid <65% SiO ₂
BA1202-10	20	2332	20	1498	18	0	0.281057	13	0.000419	0.011523	2.91	3.04	0.281034	1.99	4	N	Granitoid <65% SiO ₂
BA1202-11	20	2220	22	1679	18	<0.05	0.281082	16	0.000866	0.024600	2.91	3.04	0.281035	1.90	4	DO	Mafic rocks
BA1202-12	20	2512	22	2561	20	0	0.281076	19	0.000875	0.023869	2.92	3.07	0.281029	1.06	2	DO	Granitoid <65% SiO ₂
BA1202-13C	20	2540	20	2565	18	0	0.281061	15	0.000605	0.016997	2.92	3.05	0.281028	1.89	4	ODN	Granitoid <65% SiO ₂
BA1202-13R	20	2606	20	2595	18	0											
BA1202-15R	24	2221	24	2169	44	0.8	0.281042	13	0.000722	0.020279	2.95	3.16	0.281004	-1.06	4	OMN	Insufficient parameters
BA1202-18C	20	2528	22	2479	18	0	0.281067	17	0.000441	0.011935	2.90	3.03	0.281043	1.97	2	DO	Granitoid <65% SiO ₂

BQ1125-10	24	2726	24	2700	22	0	0.280940	30	0.000644	0.020039	3.08	3.53	0.280906	-5.48	1	O	Granitoid <65% SiO ₂
BQ1125-12	22	2690	22	1877	20	0	0.281129	36	0.000845	0.027726	2.85	2.93	0.281083	3.80	3	DO	Granitoid <65% SiO ₂
BQ1125-13	24	2773	24	2813	22	0	0.281104	30	0.000522	0.016706	2.86	2.92	0.281075	4.46	2	OD	Granitoid <65% SiO ₂
BQ1125-14	28	1791	26	921	26	<0.05	0.280998	30	0.000402	0.014342	2.98	3.12	0.280976	1.51	2	OD	Mafic rocks
BQ1125-15	24	1877	20	1827	40	0.8	0.281046	11	0.001130	0.032086	2.98	3.38	0.280993	-7.96	2	OM	Granitoid >75% SiO ₂
BQ1125-16	22	2574	22	2721	20	0	0.280977	26	0.000436	0.013371	3.01	3.23	0.280954	-1.23	3	N	Granitoid <65% SiO ₂
BQ1125-18C	26	2668	24	2660	22	0	0.280769	56	0.000446	0.013731	3.28	3.65	0.280745	-7.41	2	DO	Granitoid <65% SiO ₂
BQ1125-18R	24	2326	24	2686	22	0	0.280953	28	0.000485	0.015111	3.05	3.19	0.280926	1.15			
BQ1125-19	20	2381	18	1886	18	<0.05	0.281095	28	0.000295	0.013159	2.85	2.84	0.281078	6.80	4	OD	Ne-syenite and syenite pegmatites
BQ1125-20	20	2376	18	15577	16	0	0.281203	28	0.004609	0.157724	3.05	3.30	0.280969	-4.12	3	M	Ne-syenite and syenite pegmatites
BQ1125-21	20	1444	18	719	18	<0.05	0.281080	13	0.001850	0.047135	2.99	3.34	0.280991	-6.48	4	M	Granitoid 70–75% SiO ₂
BQ1125-22	22	2662	22	2525	22	0	0.281030	26	0.000417	0.012293	2.94	3.09	0.281007	1.51	3	N	Mafic rocks
BQ1125-23C	28	2273	24	515	26	<0.05	0.281006	58	0.000669	0.021573	2.99	3.02	0.280967	5.24	2	NO	Mafic rocks
BQ1125-23R	24	2431	22	1617	22	0	0.281081	46	0.001323	0.043645	2.95	2.89	0.281001	8.03			
BQ1125-24	20	2760	18	2546	18	0	0.280980	17	0.000410	0.013375	3.01	3.16	0.280957	0.74	2	DN	Granitoid <65% SiO ₂
BQ1125-25	22	2681	20	2675	20	0	0.281029	26	0.000671	0.020703	2.96	3.12	0.280993	0.98	4	O	Granitoid <65% SiO ₂
BQ1125-26R	26	2155	22	2086	56	2.6	0.281063	26	0.001482	0.057177	2.98	3.17	0.280984	-0.28	3	ON	
BQ1125-29	22	1771	20	1078	18	<0.05	0.281070	18	0.001789	0.048646	3.00	3.23	0.280977	-2.21	3	M	Granitoid 70–75% SiO ₂
BQ1125-30	24	1865	24	853	22	<0.05	0.281004	24	0.000511	0.016208	2.98	3.17	0.280976	-0.05	2	O	Granitoid <65% SiO ₂
BQ1125-33	24	2059	22	685	22	<0.05	0.280942	24	0.000629	0.018892	3.07	3.27	0.280907	-0.81	3	DON	Granitoid <65% SiO ₂

BQ1134-9	22	2712	20	2695	20	0	0.281066	28	0.000565	0.016130	2.91	3.05	0.281036	1.56	2	N	Granitoid <65% SiO ₂
BQ1134-10	22	2727	22	1638	20	0	0.280979	24	0.000246	0.006858	3.00	3.18	0.280966	-0.15	3	ON	Granitoid <65% SiO ₂
BQ1134-11	24	2658	22	2625	22	0	0.280936	24	0.000374	0.011359	3.06	3.32	0.280916	-2.78	4	N	Granitoid <65% SiO ₂
BQ1134-12	20	2277	20	355	20	0	0.281010	36	0.000868	0.025901	3.00	3.25	0.280964	-2.26	4	ON	Granitoid <65% SiO ₂
BQ1134-13	22	2706	22	2279	20	0	0.281123	17	0.001097	0.028986	2.87	2.97	0.281064	3.17	5	M	Granitoid <65% SiO ₂
BQ1134-14	20	2706	20	1754	20	0	0.281085	32	0.000668	0.018815	2.89	3.02	0.281049	2.03	2	N	Granitoid <65% SiO ₂
BQ1134-15	24	2614	24	2486	22	0	0.281023	24	0.000688	0.021025	2.97	3.17	0.280986	-0.47	4	ON	Granitoid <65% SiO ₂
BQ1134-16	24	2738	24	1861	24	0	0.281051	32	0.000574	0.016664	2.93	3.07	0.281020	1.69	4	N	Granitoid <65% SiO ₂

Murchison Province, Byro Sheet

BG7784-3	18	1942	16	79	20	<0.05	0.281085	14	0.001802	0.067331	2.98	3.03	0.280981	4.24	4	O	Granitoid 70–75% SiO ₂
BG7784-5	22	1524	20	1448	56	0.8	0.280995	11	0.001131	0.038238	3.04	3.46	0.280941	-8.67	3	OM	Granitoid 70–75% SiO ₂
BG7784-9	20	2967	18	3037	20	0	0.280688	19	0.000908	0.029170	3.42	3.70	0.280633	-4.94	4	N	Granitoid <65% SiO ₂
BG7784-10	20	1575	20	198	20	<0.05	0.281052	24	0.001012	0.034355	2.96	3.01	0.280994	4.52	3	DO	Granitoid 70–75% SiO ₂
BG7784-11	18	2657	18	1744	18	0	0.280989	22	0.001558	0.055901	3.09	3.32	0.280905	-2.46	4	OD	Granitoid 70–75% SiO ₂
BG7784-12	20	2661	20	2631	20	0	0.281062	17	0.000443	0.014772	2.90	3.00	0.281038	3.31	5	N	Granitoid <65% SiO ₂
BG7784-13	18	2584	18	2757	22	0	0.280994	13	0.001230	0.048553	3.05	3.20	0.280925	0.69	4	ON	Granitoid 70–75% SiO ₂
BG7784-14	18	2598	18	895	18	0	0.281040	20	0.001034	0.031285	2.98	3.06	0.280981	3.18	-	ON	Granitoid <65% SiO ₂
BG7784-15	20	2650	20	212	28	0	0.280999	18	0.000255	0.008569	2.97	3.10	0.280985	1.96	4	N	Granitoid <65% SiO ₂
BG7784-17	16	2524	16	1696	24	0	0.280987	15	0.000451	0.015952	3.00	3.14	0.280962	1.48	3	ON	Granitoid <65% SiO ₂
BG7784-18	20	2451	20	358	20	0	0.281006	18	0.000675	0.023570	2.99	3.17	0.280969	0.22	4	ON	Granitoid <65% SiO ₂

BG7784-47	18	2697	18	1565	18	0	0.280963	30	0.003798	0.155894	3.32	3.52	0.280740	-2.95	3	DO	Granitoid >75% SiO ₂
BG7784-48	18	1921	16	188	18	<0.05	0.281008	16	0.002086	0.080043	3.10	3.25	0.280889	0.38	2	MO	Granitoid 70–75% SiO ₂
BG7784-50	20	2666	18	2597	18	0	0.280929	30	0.000562	0.017258	3.08	3.32	0.280898	-2.39	4	N	Mafic rocks
BG7784-51	20	2574	20	1209	22	0	0.281076	13	0.000360	0.010593	2.88	2.95	0.281056	4.16	4	ON	Granitoid <65% SiO ₂
BG7784-53	20	2549	20	2723	20	0	0.281008	16	0.001188	0.040445	3.03	3.22	0.280943	-0.68	3	D	Granitoid 70–75% SiO ₂
BG7784-54	20	2417	20	2212	20	0	0.280841	20	0.001251	0.041310	3.26	3.46	0.280767	-1.85	4	DO	Granitoid 70–75% SiO ₂
BG7784-55	18	2704	16	349	18	0	0.280982	19	0.001283	0.052024	3.07	3.29	0.280912	-1.74	4	D	Granitoid 70–75% SiO ₂
BG7784-56	18	1772	18	275	18	<0.05	0.280907	22	0.001700	0.063771	3.21	3.28	0.280802	2.77	3	DM	Mafic rocks
BG7784-57	18	2260	18	142	18	<0.05	0.280854	18	0.001195	0.051271	3.23	3.33	0.280781	1.81	3	N	Granitoid 70–75% SiO ₂
BG7784-58	20	1988	20	1985	20	0.19	0.281012	15	0.001835	0.062068	3.08	3.35	0.280915	-3.90	2	N	Granitoid 70–75% SiO ₂
BG7784-59	20	2688	20	2703	18	0	0.281008	17	0.001190	0.038064	3.03	3.22	0.280943	-0.64	3	D	Granitoid 70–75% SiO ₂
BG7784-60	20	2932	20	962	20	0	0.280889	15	0.000490	0.013043	3.13	3.23	0.280860	2.33	3	ON	Granitoid <65% SiO ₂
BG7784-61	18	2720	18	1964	20	0	0.281000	17	0.000355	0.011498	2.98	3.13	0.280981	1.08	4	DN	Granitoid <65% SiO ₂

Narryer Province, Robinson Range Sheet

BA1471-1	16	1271	18	1013	18	<0.05	0.281195	20	0.004965	0.180024	3.09	3.46	0.280966	-9.77	4	M	Ne-syenite and syenite pegmatites
BA1471-2	16	2415	16	1773	18	0	0.280842	12	0.001618	0.047973	3.29	3.61	0.280752	-6.28	3	O	Granitoid 70–75% SiO ₂
BA1471-2R	16	2184	16	2153	62	0.3	0.281068	14	0.001373	0.047177	2.97	3.28	0.281000	-4.79			
BA1471-3	16	1477	18	838	18	<0.05	0.281098	16	0.001361	0.047680	2.93	3.32	0.281035	-7.54	4	M	Granitoid 70–75% SiO ₂
BA1471-4	22	1572	22	1499	84	0.5	0.281054	13	0.001009	0.034662	2.96	3.28	0.281005	-5.11	3	MO	Granitoid 70–75% SiO ₂
BA1471-5	22	2330	22	2851	26	0	0.281066	16	0.000964	0.034300	2.94	3.13	0.281015	-0.33	4	N	Granitoid 70–75% SiO ₂

BA1471-46	52	1766	22	1685	440	14	0.281134	16	0.002048	0.076/34	2.93	3.28	0.281038	-6.42	3	M	Granitoid	70–75% SiO ₂
BA1471-47	16	2552	16	2702	18	0	0.280859	13	0.000422	0.013598	3.16	3.51	0.280837	-6.16	4	N	Granitoid	<65% SiO ₂
BA1471-48	20	1432	16	1391	74	2.6	0.281180	16	0.003048	0.111021	2.95	3.54	0.281067	-16.87	4	OM	Granitoid	70–75% SiO ₂
BA1471-49	14	2605	14	2969	18	0	0.281060	9	0.001255	0.043256	2.97	3.17	0.280994	-0.99	4	DN	Granitoid	70–75% SiO ₂
BA1471-50	14	1243	14	1166	98	0.6	0.281079	17	0.001795	0.062126	2.99	3.47	0.281001	-11.62	4	M	Granitoid	70–75% SiO ₂
BA1471-52	18	2505	18	2713	24	0	0.281050	8	0.000890	0.030521	2.95	3.11	0.281002	0.81	3	MN	Granitoid	70–75% SiO ₂
BA1471-53	16	1838	14	1957	20	0	0.281461	12	0.000361	0.010870	2.38	2.76	0.281448	-4.66	4	N	Granitoid	<65% SiO ₂
BA1471-55	16	2599	16	2836	18	0	0.280855	19	0.000807	0.026659	3.20	3.59	0.280813	-8.01	3	OD	Granitoid	<65% SiO ₂
BA1471-56	14	2472	14	2512	18	0	0.280857	17	0.000420	0.015766	3.17	3.52	0.280835	-6.41	4	OD	Granitoid	<65% SiO ₂
BA1471-57	16	1497	16	794	18	<0.05	0.281053	8	0.000884	0.028683	2.95	3.36	0.281012	-8.04	4	OM	Granitoid	70–75% SiO ₂
BA1471-58	14	1665	14	1444	18	<0.05	0.281064	11	0.001490	0.048303	2.98	3.41	0.280996	-9.23	4	M	Granitoid	70–75% SiO ₂
BA1471-59	18	1205	16	1127	128	1.8	0.281057	19	0.003136	0.132126	3.13	3.79	0.280938	-20.50	4	DMO	Granitoid	70–75% SiO ₂
BA1471-59R	20	1285	16	1195	182	2.6	0.281056	24			2.88	3.38	0.281056	-10.57				

Capricorn Orogen, Mt. Egerton Sheet

BA5127-2	18	2242	18	2308	18	0	0.281252	15	0.000326	0.010286	2.65	2.93	0.281238	-2.10	5	D	Granitoid	<65% SiO ₂
BA5127-3	18	1764	18	1857	18	0	0.281419	9	0.000979	0.029864	2.48	2.91	0.281384	-7.39	5	N	Granitoid	70–75% SiO ₂
BA5127-4	18	1842	18	1922	18	0	0.281510	13	0.000191	0.006183	2.31	2.62	0.281503	-2.14	5	N	Carbonatite	
BA5127-5	20	1776	20	1595	20	0	0.281435	26	0.000292	0.010202	2.41	2.82	0.281425	-5.91	4	N	Granitoid	<65% SiO ₂
BA5127-6	18	2429	20	2376	18	0	0.281060	14	0.000796	0.027749	2.93	3.21	0.281020	-3.22	4	N	Granitoid	70–75% SiO ₂
BA5127-7	16	1841	16	1845	16	0	0.281421	12	0.000702	0.023712	2.45	2.86	0.281395	-6.05	4	OD	Granitoid	<65% SiO ₂
BR1673-1	22	1794	22	1834	22	0	0.281433	9	0.000334	0.011244	2.42	2.79	0.281421	-4.57	4	N	Granitoid	<65% SiO ₂

J8272-16	26	1750	20	1855	26	0	0.281594	20	0.000190	0.000115	2.40	2.70	0.281587	7.65	4	DN	Carbonatite
J8272-17	22	1739	22	1760	22	0	0.281461	15	0.000443	0.013446	2.39	2.78	0.281445	-5.27	3	N	Granitoid <65% SiO ₂
J8272-18	18	1735	20	1780	18	0	0.281388	14	0.000463	0.013016	2.48	2.95	0.281372	-8.26	4	N	Granitoid <65% SiO ₂
J8272-19	18	2185	20	2309	20	0	0.281250	20	0.000347	0.010288	2.65	2.96	0.281235	-3.10	4	N	Granitoid <65% SiO ₂
J8272-20	20	1767	22	1800	20	0	0.281396	18	0.000153	0.004736	2.45	2.90	0.281391	-7.38	4	ON	Carbonatite
J8272-21	20	1774	22	1816	20	0	0.281456	12	0.000520	0.015305	2.40	2.80	0.281438	-5.59	3	N	Granitoid <65% SiO ₂
J8272-22	22	1761	22	1871	22	0	0.281472	19	0.000343	0.010719	2.37	2.75	0.281460	-4.96	3	O	Granitoid <65% SiO ₂
J8272-23	22	1761	24	1831	22	0	0.281457	17	0.000463	0.015248	2.39	2.80	0.281441	-5.83	4	DO	Granitoid <65% SiO ₂
J8272-24	30	1680	20	1672	36	0.5	0.281507	12	0.000331	0.010531	2.32	2.71	0.281496	-4.80	4	DN	Granitoid <65% SiO ₂
J8272-25	18	2111	20	2164	20	0	0.281209	14	0.000077	0.002983	2.69	3.07	0.281206	-5.74	4	DN	Carbonatite
J8272-26	28	1409	24	1388	58	1.0	0.281330	20	0.000543	0.020396	2.56	3.15	0.281312	-12.94	3	DO	Granitoid <65% SiO ₂
J8272-27	18	2058	18	2017	18	0	0.281276	17	0.000153	0.004780	2.61	2.85	0.281269	-0.81	4	N	Carbonatite
J8272-28	16	2143	18	1792	18	0	0.281292	12	0.000492	0.015683	2.61	2.85	0.281270	-0.63	5	OD	Granitoid <65% SiO ₂

^a C: core; R: rim; D: dark; L: light; A: duplicate.^b O: concordant, or consistent single-stage Pb-loss pattern, no correction.^c 1: euhedral to 5: rounded.^d O: oscillatory; D: diffuse; L: laminated; N: no zoning; M: metamict. In order from less important to predominant.

References

- Amelin, Y., Lee, D.-C., Halliday, A.N., Pidgeon, R.T., 1999. Nature of the Earth's earliest crust from hafnium isotopes in single detrital zircons. *Nature* 399, 252–255.
- Andersen, T., 2002. Correction of common Pb in U–Pb analyses that do not report ^{204}Pb . *Chem. Geol.* 192, 59–79.
- Bagas, L., 1999. Early tectonic history of the Marymia Inlier and correlation with the Archaean Yilgarn Craton, Western Australia. *Aust. J. Earth Sci.* 46, 115–125.
- Belousova, E., Griffin, W.L., O'Reilly, S.Y., 1999. Cathodoluminescence and geochemical properties of kimberlitic and lamproitic zircons. In: Proceedings of Seventh International Kimberlite Conference, Red Roof Design, Cape Town, pp. 23–29.
- Belousova, E.A., Griffin, W.L., Shee, S.R., Jackson, S.E., O'Reilly, S.Y., 2001. Two age populations of zircons from the Timber Creek kimberlites, Northern Territory, Australia, as determined by laser ablation-ICPMS analysis. *Aust. J. Earth Sci.* 48, 757–766.
- Belousova, E.A., Griffin, W.L., O'Reilly, S.Y., Fisher, N.I., 2002. Trace element composition of zircon: relationship to host rock type. *Contrib. Mineral. Petrol.* 143, 602–622.
- Bizzarro, M., Baker, J.A., Haack, H., Ulfbeck, D., Rosing, M., 2003. Early history of Earth's crust–mantle system inferred from hafnium isotopes in chondrites. *Nature* 421, 931–933.
- Black, L.P., Gulson, B.L., 1978. The age of the Mud Tank carbonatite, Strangways Range, Northern Territory. *BMR J. Aust. Geol. Geophys.* 3, 227–232.
- Blichert-Toft, J., Chauvel, C., Albarède, F., 1997. The Lu–Hf geochemistry of chondrites and the evolution of the mantle–crust system. *Earth Planet. Sci. Lett.* 148, 243–258. Erratum *Earth Planet. Sci. Lett.* 154 (1998), 349.
- Breiman, L., Friedman, J.H., Olshen, R.A., Stone, C.J., 1984. Classification and Regression Trees. Wadsworth, CA, 358 pp.
- Champion, D.C., 1997. Granitoids in the eastern Goldfields. *Aust. Geol. Surv. Org. Rec.* 41, 71–75.
- Champion, D.C., Sheraton, J.W., 1997. Geochemistry and Nd isotope systematics of Archaean granites of the Eastern Goldfields, Yilgarn Craton, Australia: implications for crustal growth processes. *Precambrian Res.* 83, 109–132.
- Gee, R.D., 1979. Structure and tectonic style of the Western Australian shield. *Tectonophysics* 58, 327–369.
- Graham, S., Lambert, D.D., Shee, S.R., Smith, C.B., Hamilton, R., 1999. Re–Os and Sm–Nd isotopic constraints on the sources of kimberlites and melnoites, Earaheedy Basin, Western Australia. In: Proceedings of Seventh International Kimberlite Conference, Red Roof Design, Cape Town, pp. 280–290.
- Griffin, W.L., Pearson, N.J., Belousova, E., Jackson, S.E., O'Reilly, S.Y., van Achterberg, E., Shee, S.R., 2000. The Hf-isotope composition of cratonic mantle: LAM-MC-ICPMS analysis of zircon megacrysts in kimberlites. *Geochim. Cosmochim. Acta* 64, 133–147.
- Griffin, W.L., Wang, X., Jackson, S.E., Pearson, N.J., O'Reilly, S.Y., Xu, X., Zhou, X., 2002. Zircon chemistry and magma genesis, SE China: in-situ analysis of Hf isotopes, Pingtan and Tonglu igneous complexes. *Lithos* 61, 237–269.
- Hall, C.E., McPowell, C.A., Bryant, J., 2001. Basin setting and age of the late Paleoproterozoic Capricorn formation, Western Australia. *Aust. J. Earth Sci.* 48, 731–744.
- Hamilton, R., Rock, N.M., 1990. Geochemistry, mineralogy and petrology of a new find of ultramafic lamprophyres from Bulljah Pool, Nabberu Basin, Yilgarn Craton, Western Australia. *Lithos* 24, 275–290.
- Hoskin, P.W.O., Black, L.P., 2000. Metamorphic zircon formation by solid-state recrystallization of protolith igneous zircons. *J. Metamorphic Geol.* 18, 423–439.
- Hoskin, P.W.O., Ireland, T.R., 2000. Rare earth element chemistry of zircon and its use as a provenance indicator. *Geology* 28, 627–630.
- Jackson, S.E., Pearson, N.J., William, L., Griffin, W.L., Belousova, E.A., submitted for publication. The application of laser ablation microprobe-inductively coupled plasma-mass spectrometry (LAM-ICP-MS) to in situ U–Pb zircon geochronology. *Chem. Geol.*
- Ketchum, J.W.F., Jackson, S.E., Culshaw, N.G., Barr, S.M., 2001. Depositional and tectonic setting of the Paleoproterozoic Lower Ailik Group, Makkovik Province, Canada: evolution of a passive margin-foredeep sequence based on petrochemistry and U–Pb (TIMS and LAM-ICP-MS) geochronology. *Precambrian Res.* 105, 331–356.
- Krapez, B., Brown, S.J.A., Hand, J., Barley, M.E., Cas, R.A.F., 2000. Age constraints on recycled crustal and supracrustal sources of Archaean metasedimentary sequences, Eastern Goldfields Province, Western Australia: evidence from SHRIMP zircon dating. *Tectonophysics* 322, 89–133.
- Ludwig, K.R., 2000. Isoplot/Ex version 2.3. A Geochronological Toolkit for Microsoft Excel. Berkeley Geochronology Center, Special Publication No. 1a, Berkeley.
- Myers, J.S., 1993. Precambrian history of the West Australian craton and adjacent orogens. *Ann. Rev. Earth Sci.* 21, 453–485.
- Nelson, D.R., 1997a. SHRIMP U–Pb zircon chronological constraints on the evolution of the Eastern Goldfields granite–greenstone terranes. *Aust. Geol. Surv. Org. Rec.* 41, 11–14.
- Nelson, D.R., 1997b. Evolution of the Archaean granite–greenstone terranes of the Eastern Goldfields, Western Australia: SHRIMP U–Pb zircon constraints. *Precambrian Res.* 83, 57–81.
- Norman, M.D., Pearson, N.J., Sharma, A., Griffin, W.L., 1996. Quantitative analysis of trace elements in geological materials by laser ablation ICPMS: instrumental operating conditions and calibration values of NIST glasses. *Geostandards Newslett.* 20 (2), 247–261.
- Nutman, A.P., Bennett, V.C., Kinny, P.D., Price, R., 1993. Large-scale crustal structure on the northwestern Yilgarn Craton, Western Australia: evidence from Nd isotopic data and zircon geochronology. *Tectonics* 12, 971–981.
- Nutman, A.P., 2001. On the scarcity of >3900 Ma detrital zircons in ≥ 3500 Ma metasediments. *Precambrian Res.* 105, 93–114.
- Occipinti, S.A., Sheppard, S., Nelson, D.R., Myers, J.S., Tyler, I.M., 1998. Syntectonic granite in the southern margin of the Palaeoproterozoic Capricorn Orogen, Western Australia. *Australian J. Earth Sci.* 45, 509–512.
- Patchett, P.J., Kouvo, O., Hedge, C.E., Tatsumoto, M., 1981. Evolution of continental crust and mantle heterogeneity:

- evidence from Hf isotopes. *Contrib. Mineral. Petrol.* 78, 279–297.
- Rubatto, D., Gebauer, D., Compagnoni, R., 1999. Dating of eclogite-facies zircons: the age of Alpine metamorphism in the Sesia-Lanzo Zone (Western Alps). *Earth Planet Sci. Lett.* 167, 141–158.
- Scherer, E., Munker, C., Mezger, K., 2001. Calibration of the Lutetium–Hafnium clock. *Science* 293, 683–687.
- Schiøtte, L., Campbell, I.H., 1996. Chronology of the Mount Magnet granite–greenstone terrain, Yilgarn Block, Western Australia: implication for field based prediction of the relative timing of granitoid emplacement. *Precambrian Res.* 78, 237–260.
- Shee, S.R., Vercoe, S.C., Wyatt, B.A., Campbell, A.N., Colgan, E.A., 1998. Discovery and geology of the Nabberu kimberlite province, Western Australia. In: Proceedings of Seventh International Kimberlite Conference, pp. 764–773.
- Smith, P.E., Tatsumoto, M., Farquhar, R.M., 1987. Zircon Lu–Hf systematics and the evolution of the Archean crust in the southern Superior Province. *Can. Contrib. Mineral. Petrol.* 97, 93–104.
- Stacey, J.S., Kramers, J.D., 1975. Approximation of terrestrial lead isotope evolution by a two-stage model. *Earth Planet. Sci. Lett.* 26, 207–221.
- Thirlwall, M.F., Walder, A.J., 1995. In situ hafnium isotope ratio analysis of zircon by inductively coupled plasma multiple collector mass spectrometry. *Chem. Geol.* 122, 241–247.
- Vervoort, J.D., Patchett, P.J., 1996. Behaviour of hafnium and neodymium isotopes in the crust: constraints from Precambrian crustally derived granites. *Geochim. Cosmochim. Acta* 60, 3717–3733.
- Wang, Q., Campbell, I.H., Shiøtte, L., 1996. Age constraint on the supracrustal sequence in the Murchison Province, Yilgarn Block—a new insight from the SHRIMP zircon dating. *Geol. Soc. Aust. Abst.* 41, 458.
- Wang, Q., Shiøtte, L., Campbell, I.H., 1998. Geochronology of supracrustal rocks from the Golden Grove area, Murchison Province, Yilgarn Craton, Western Australia. *Aust. J. Earth Sci.* 45, 571–577.
- Whitaker, A.J., 2001. Components and structure of the Yilgarn Craton, as interpreted from aeromagnetic data. In: Proceedings of Fourth International Archaean Symposium Ext. Abstracts AGSO-Geoscience Australia Record, vol. 37, 2001, pp. 536–538.
- Wiedenbeck, M., Watkins, K.P., 1993. A time scale for granitoid emplacement in the Archaean Murchison Province, Western Australia by single zircon geochronology. *Precambrian Res.* 61, 1–26.
- Wiedenbeck, M., Alle, P., Corfu, F., Griffin, W.L., Meier, M., Oberli, F., Von Quadt, A., Roddick, J.C., Spiegel, W., 1995. Three natural zircon standards for U–Th–Pb, Lu–Hf, trace element and REE analyses. *Geostandards Newslett.* 19, 1–24.
- Wilde, S.A., Valley, J.W., Peck, W.H., Graham, C.M., 2001. Evidence from detrital zircons for the existence of continental crust and oceans on the Earth 4.4 Gyr ago. *Nature* 409, 175–178.